Virtual Outcrop Models

Examples of application

The context in which VOMs can be used in Geology are many and are increasing.

This is happening because 3D models are becoming ever easier to realize

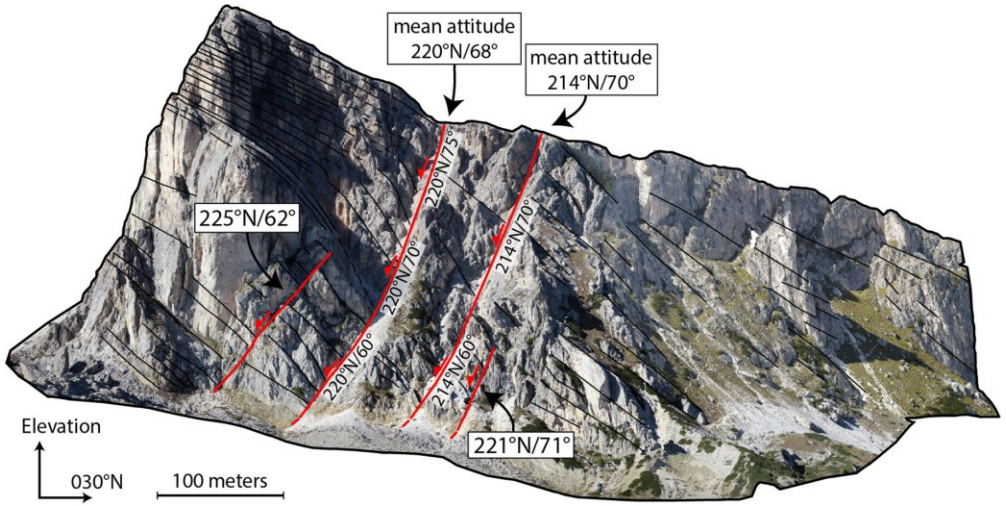

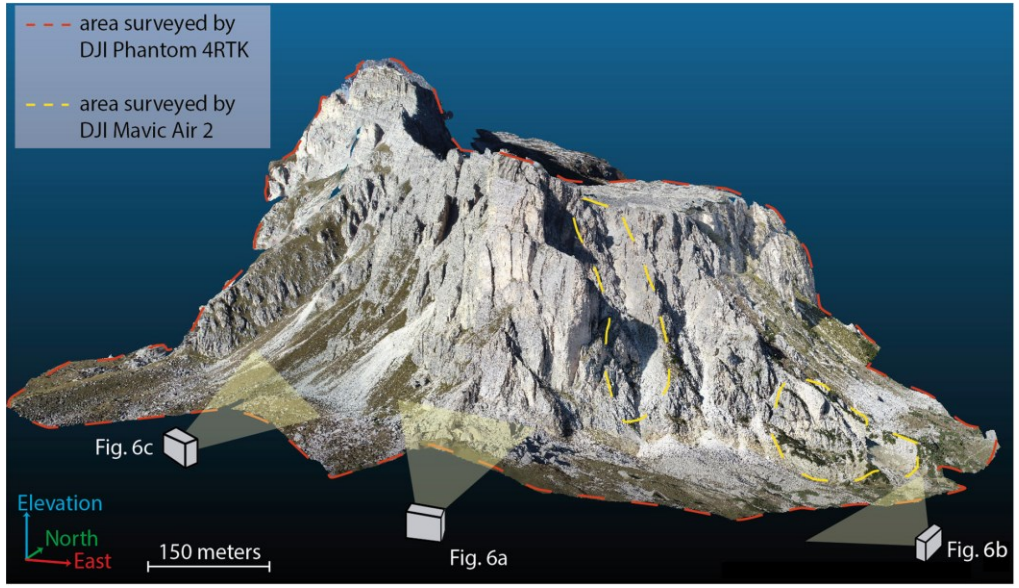

From Menegoni et al., 2022

Some tipes of possible uses of a VOM are

Extraction Structural measurements (e.g. fracture and bedding orientation)

Extraction of other geometrical features (e.g. depositional surfaces)

Facies mapping

Integration of other data (e.g. hyperspectral imaging)

Example 1: Syndepositional fracturing and architecture of a carbonate platform

The Lastoni di Formin are made of Triassic shallow water carbonates belonging to the Cassian Dolomite formation.

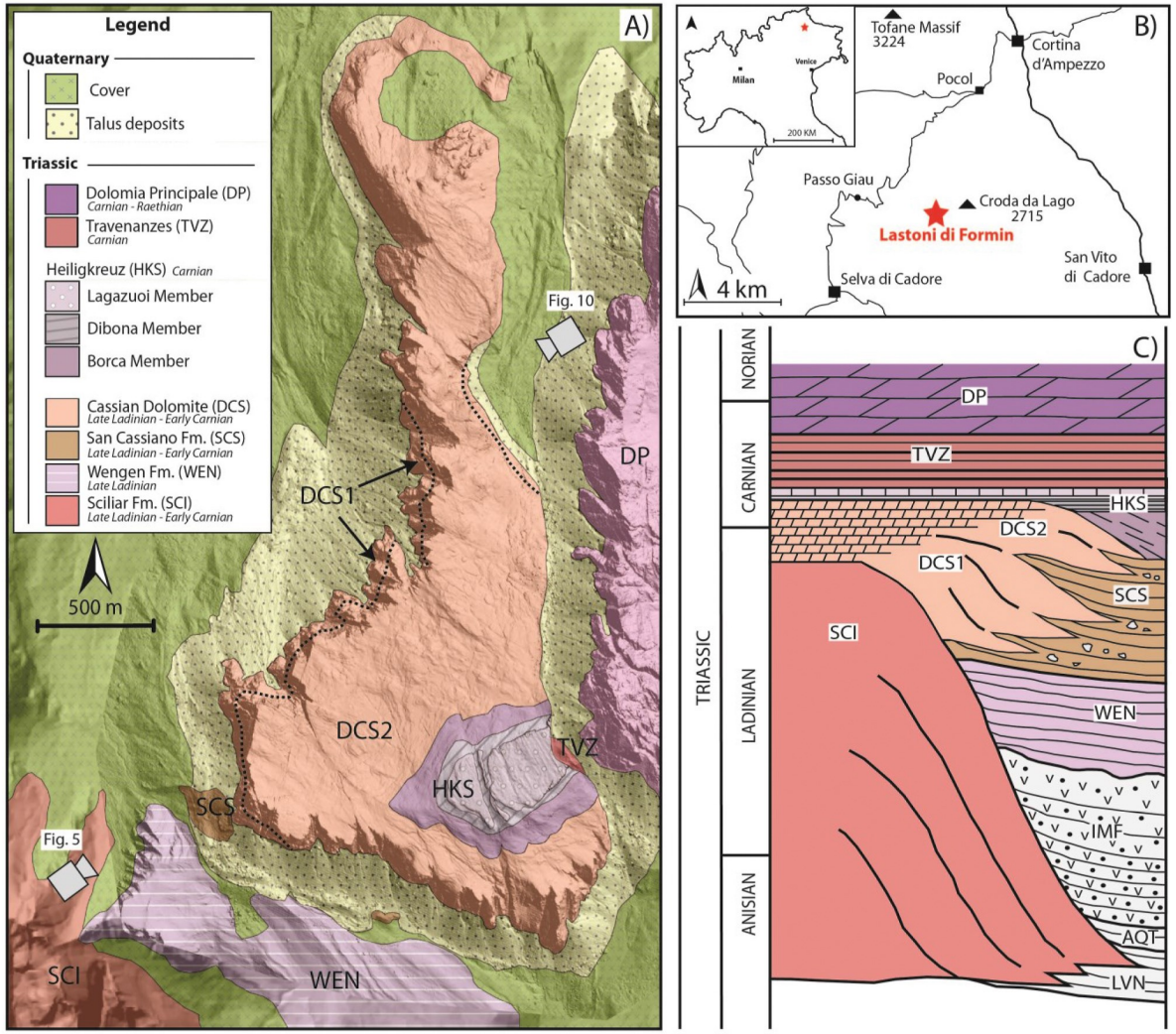

Inama et al., 2021

Example 1: Syndepositional fracturing and architecture of a carbonate platform

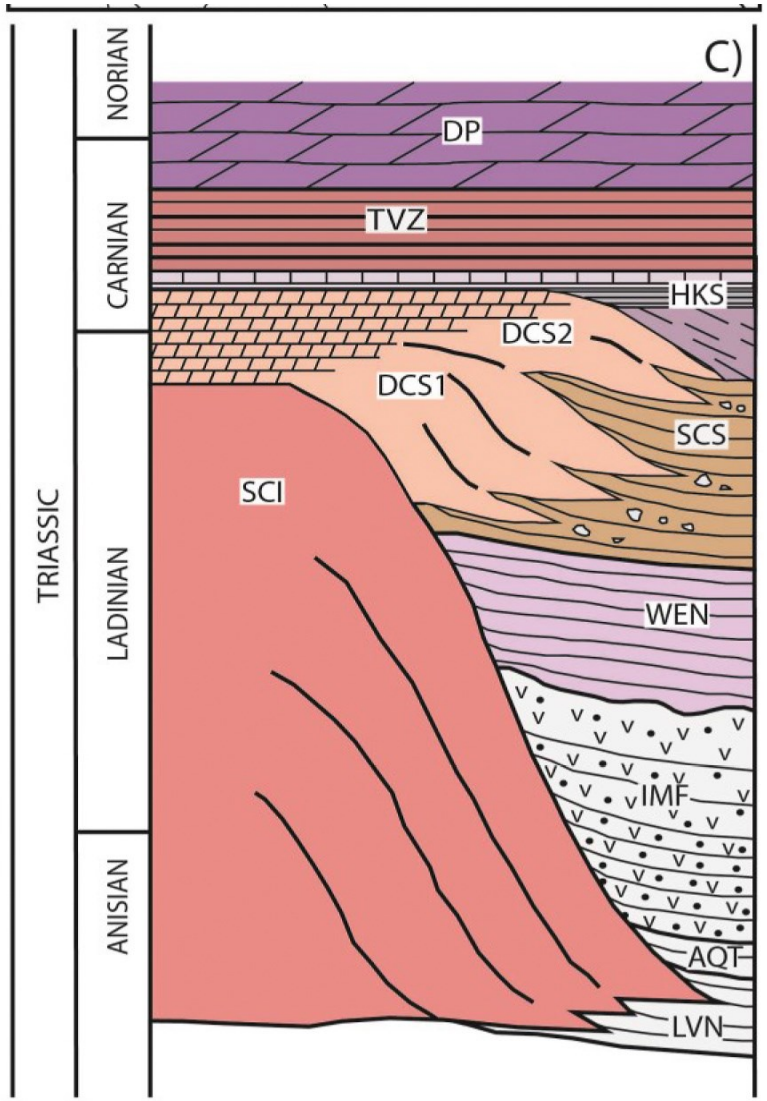

Inama et al., 2021

The Cassian Dolomite (DCS1 and DCS2) is made of dolomitized shallow water carbonates depostited on a high-relief carbonate platform and interfingers with the San Cassiano Formation (SCS) that cosists of shales and marls alternating with volcanoclastic material. In the San Cassiano Formation carbonate boulders of variable size can be found that represent olistoliths of mass transport deposits coming from the adjacent platform.
The Heiligkreuz Formation (HKS) covers both the Cassian Dolomite and the San Cassiano Formation and is made of mixed carbonate/siliciclastic rocks.

Example 1: Syndepositional fracturing and architecture of a carbonate platform

The outcrop is about 1.5 X 3 km and features vertical walls several hunderd meters-high that cannot be easily accessed

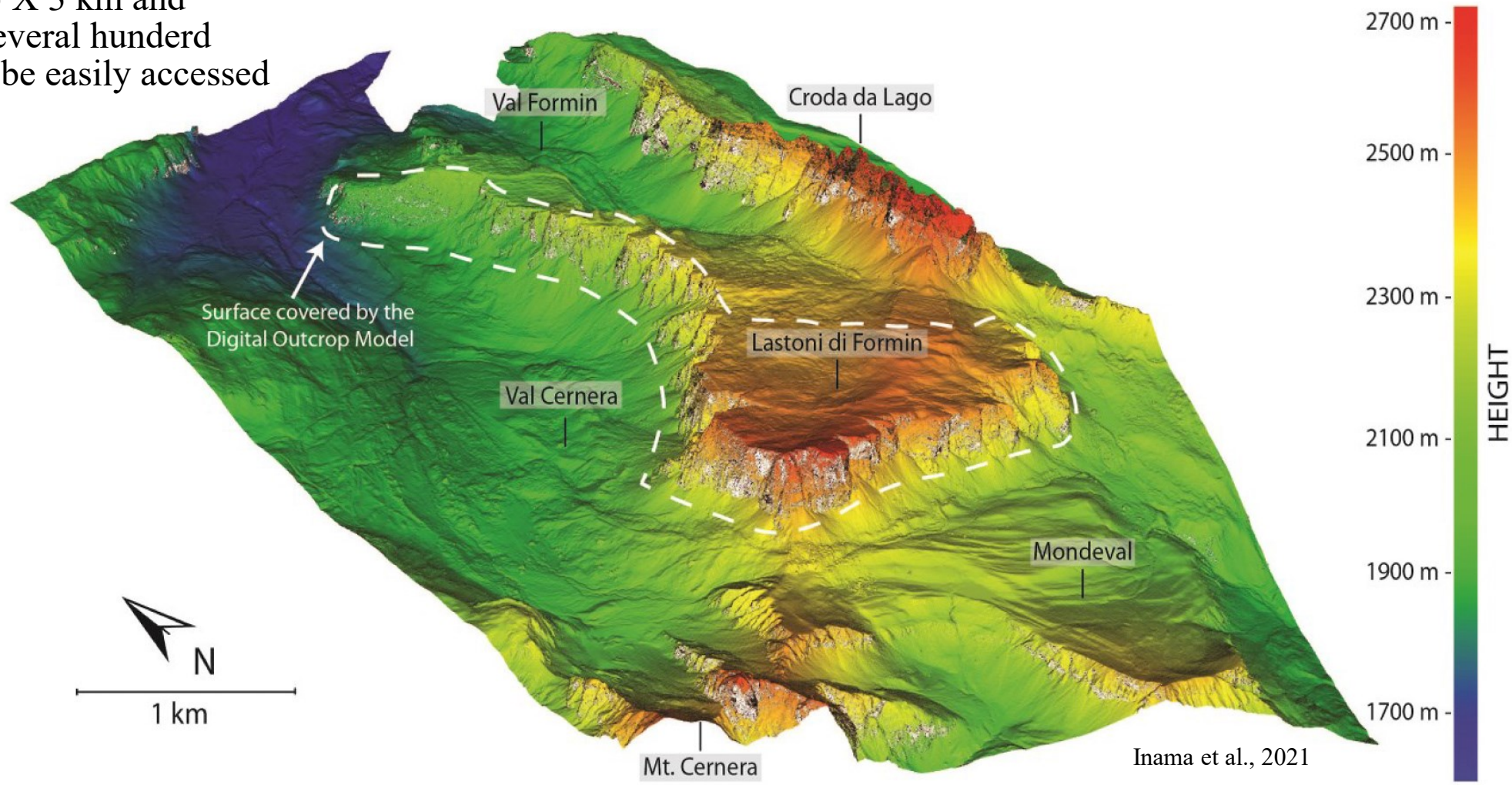

Inama et al., 2021

Example 1: Syndepositional fracturing and architecture of a carbonate platform

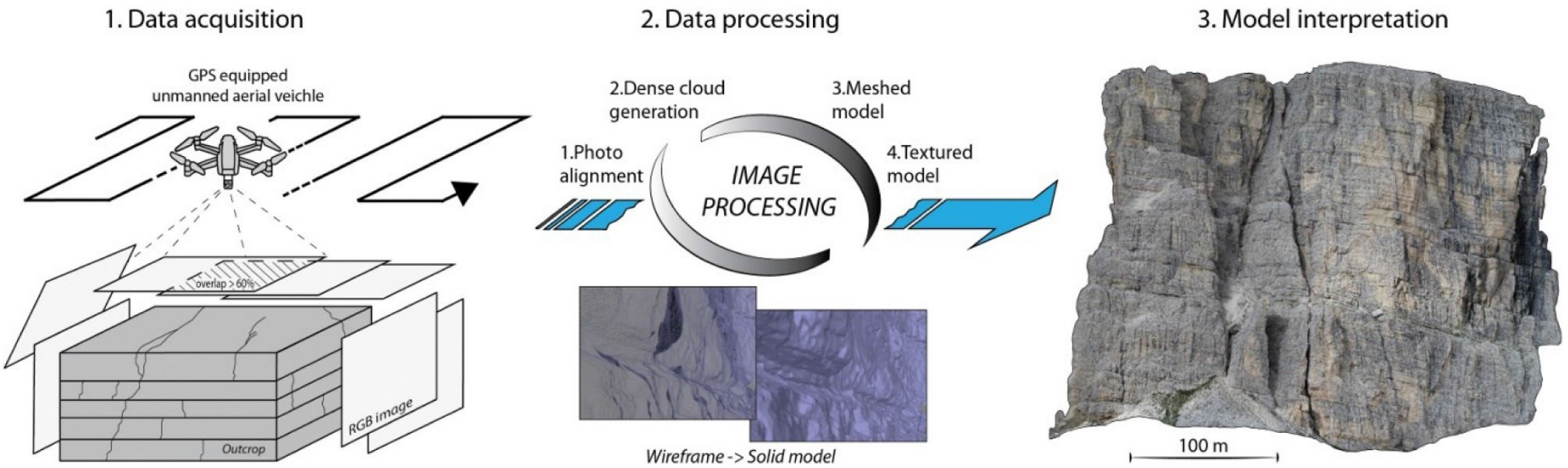

Inama et al., 2021

Example 1: Syndepositional fracturing and architecture of a carbonate platform

Direction of progradation of the Cassian Dolomite platform

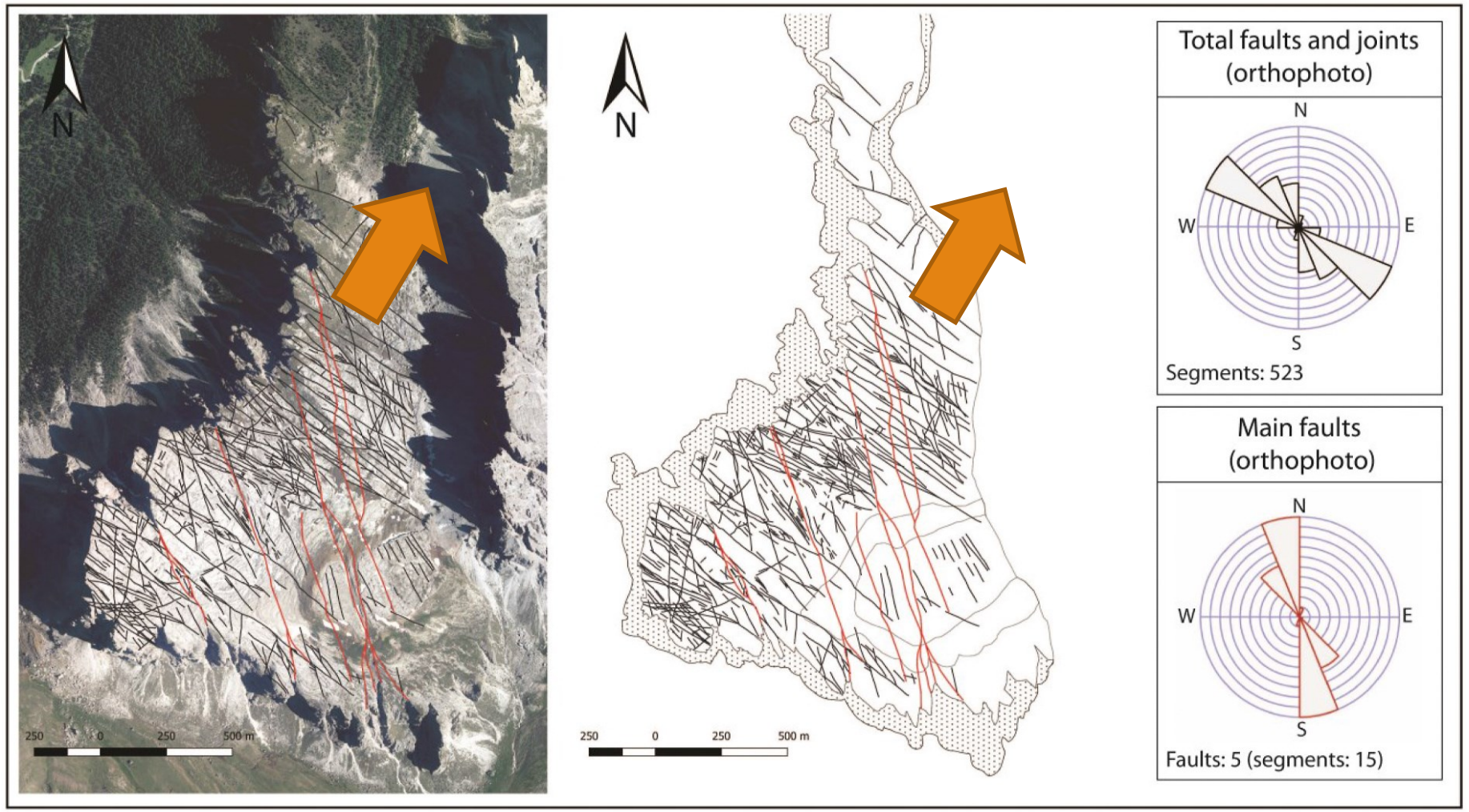

Inama et al., 2021

Example 1: Syndepositional fracturing and architecture of a carbonate platform

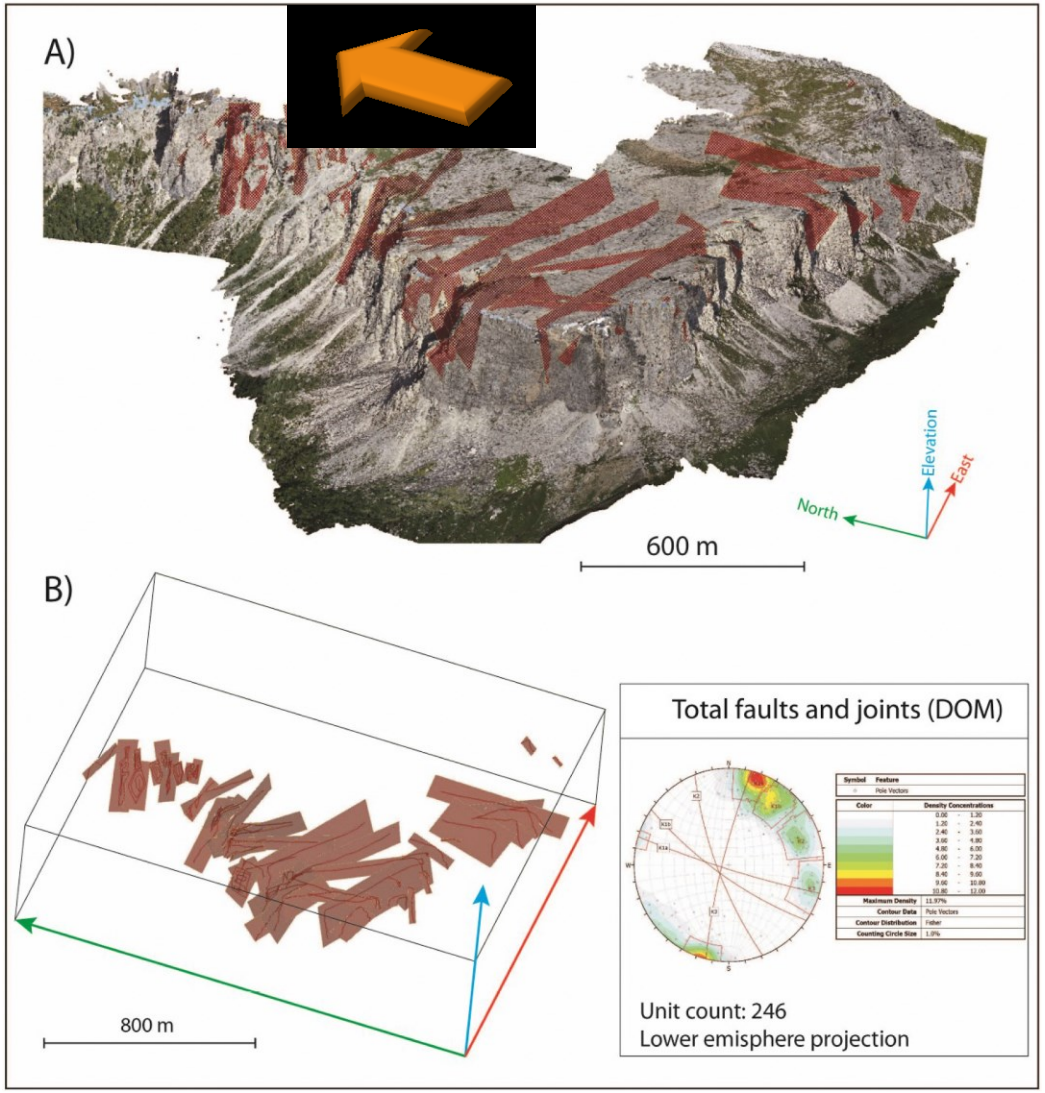

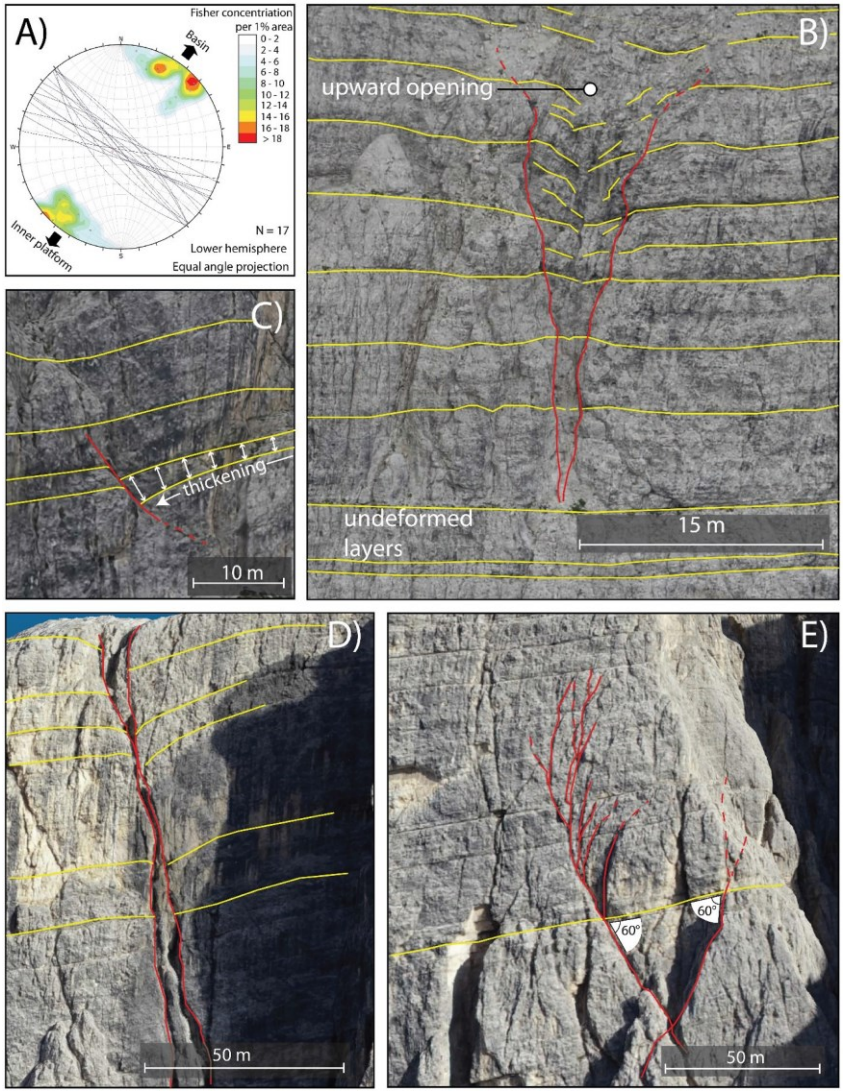

Inama et al., 2021

Example 1: Syndepositional fracturing and architecture of a carbonate platform

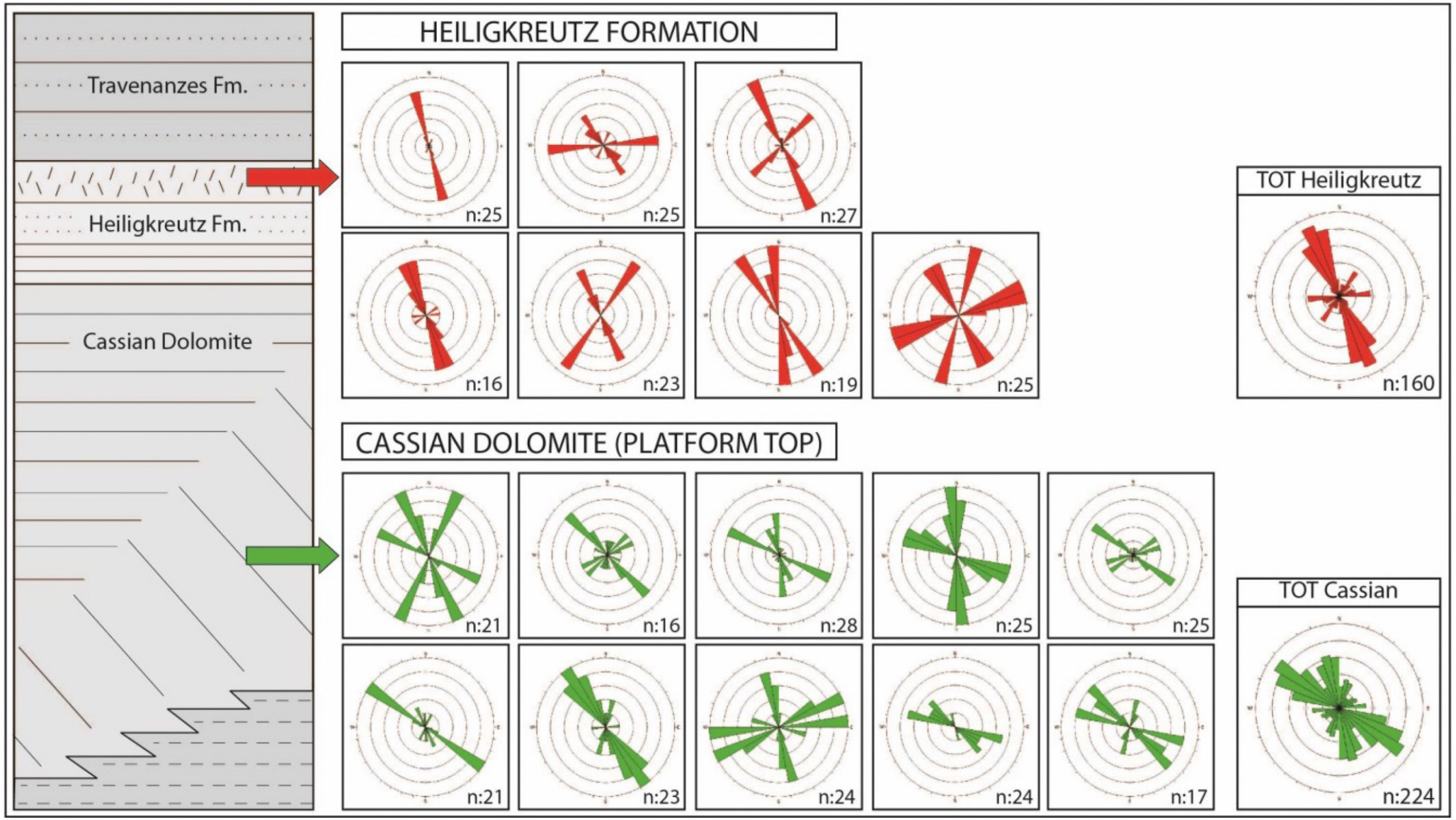

Inama et al., 2021

Example 1: Syndepositional fracturing and architecture of a carbonate platform

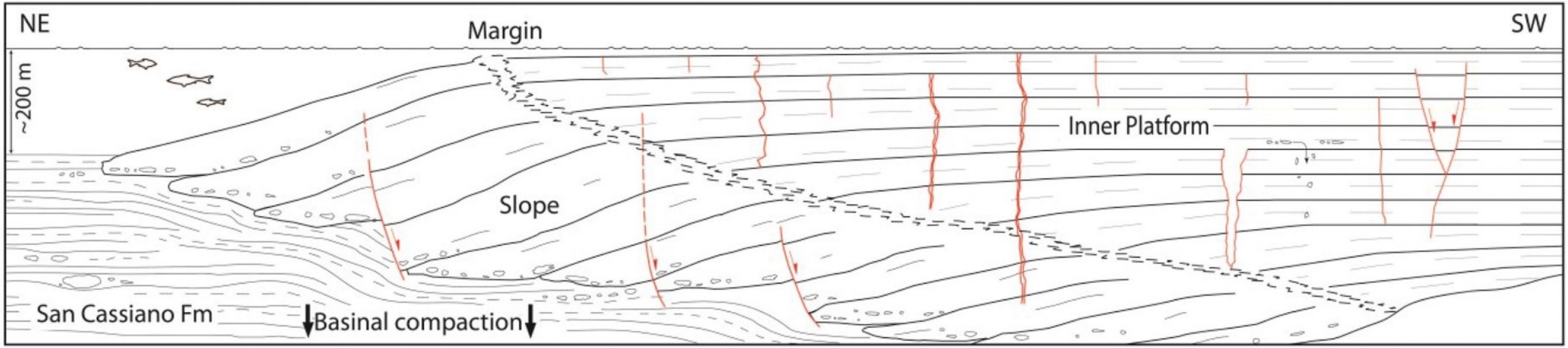

Syndepositional fractures that are orthogonal to the direction of progradation are interpreted as due to differential compaction of the more compressible basinal sediments of the San Cassiano Formation caused by the increment in load due to the progradation of the Cassian Dolomite carbonate platform.

Inama et al., 2021

Example 2: Hyperspectral imaging

VOM can be associated to hyperspectral imaging. In this example from Thiele et al. (2022), hyperspectral imaging was acquired on the outcrop of the Lastoni di Formin with the purpose of mapping in 3D variations in minearlogical characteristics of the rocks.

Below: . UAV and Hyspex Mjolnir-VS mounted sideways in the Gremsy gStabi H16 XL gimbal.

Thiele et al., 2022

Example 2: Hyperspectral imaging

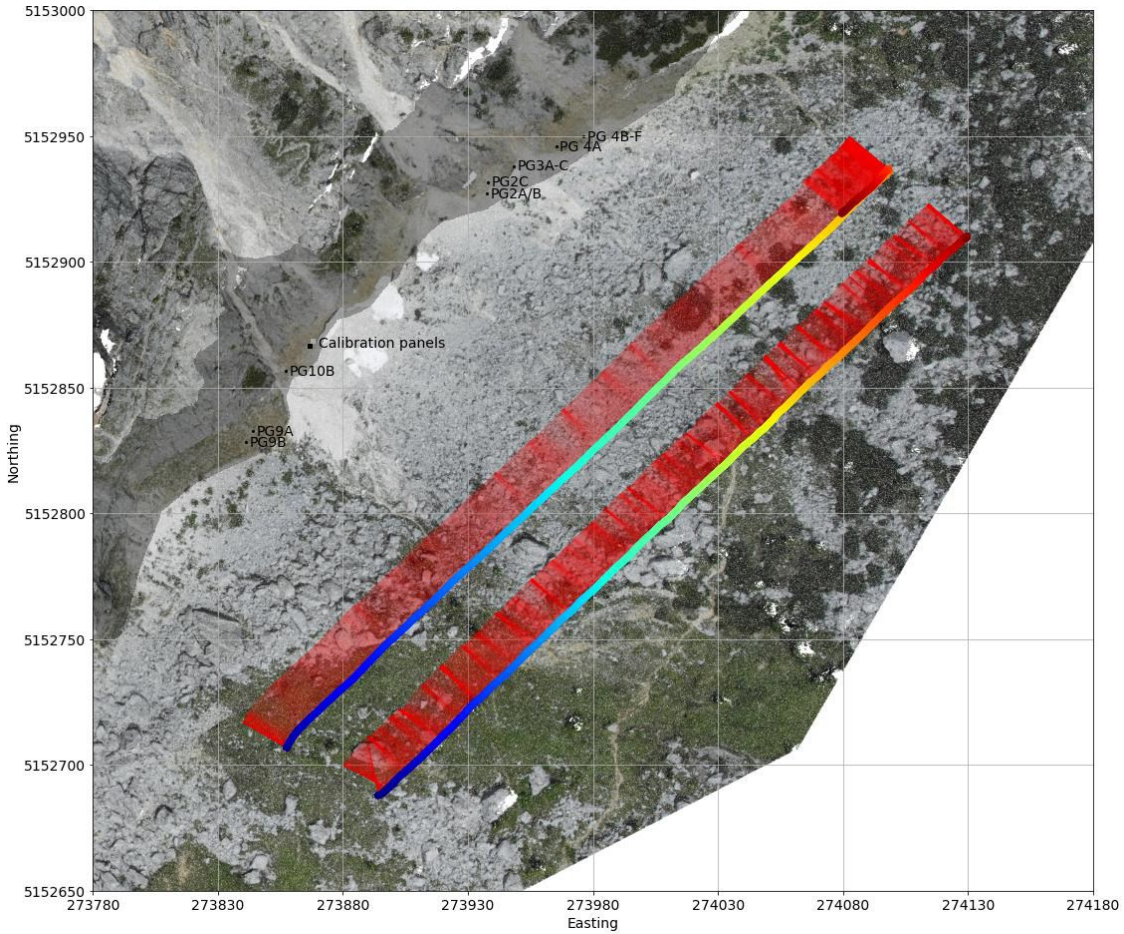

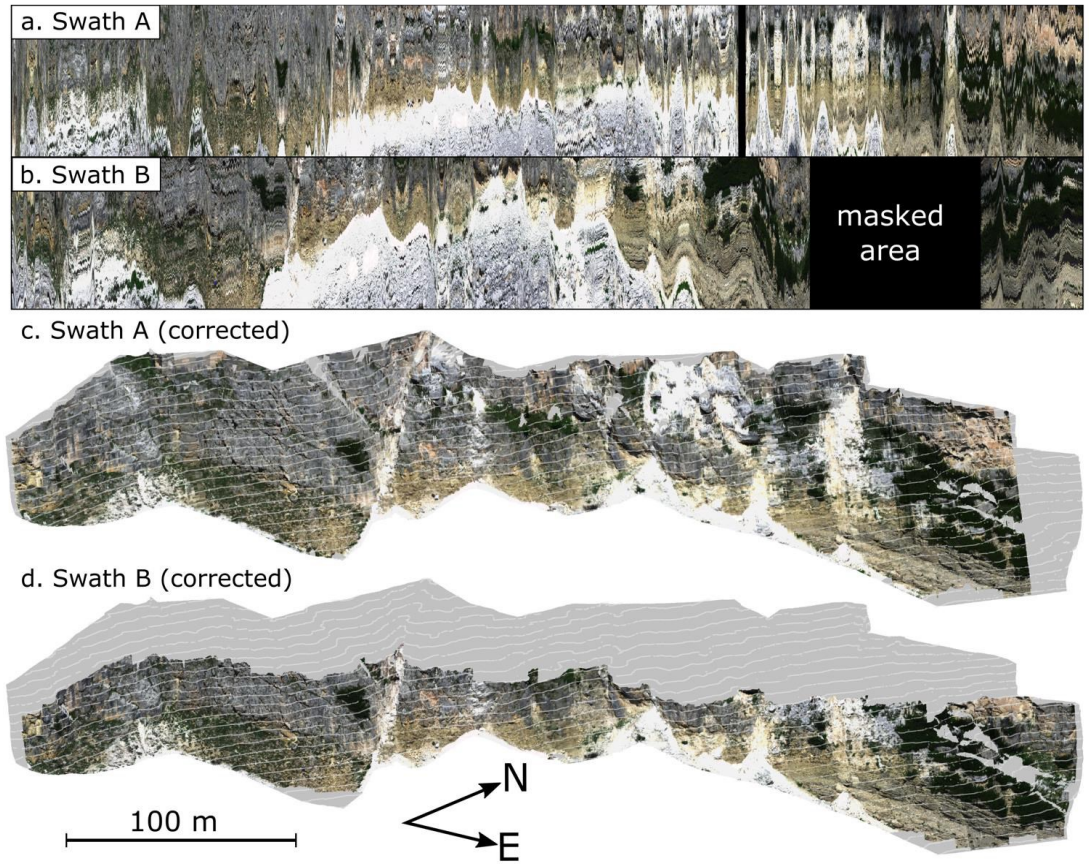

Thiele et al., 2022

Thiele et al. (2022) propose a method for geometric calibration of the hyperspectral data on the VOM.

Example 2: Hyperspectral imaging

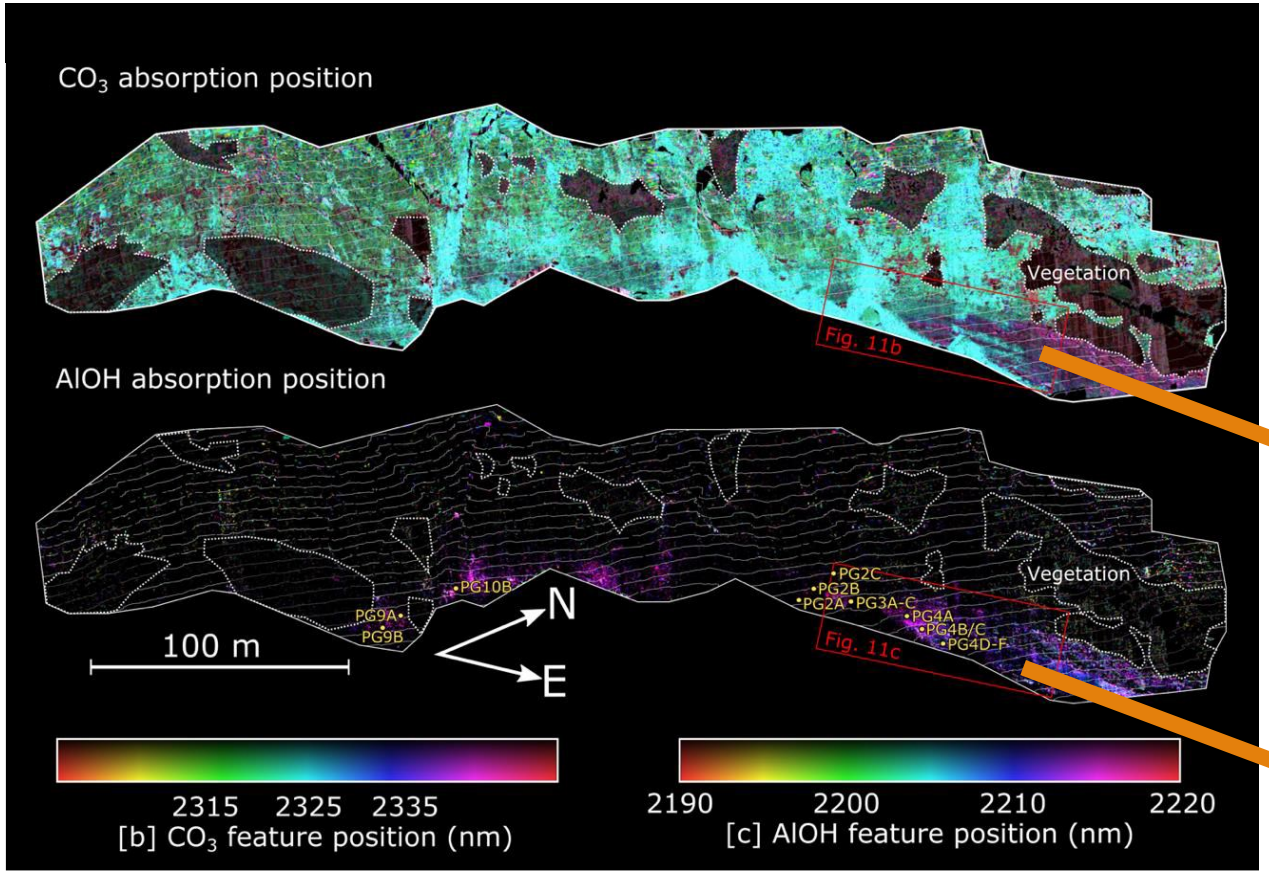

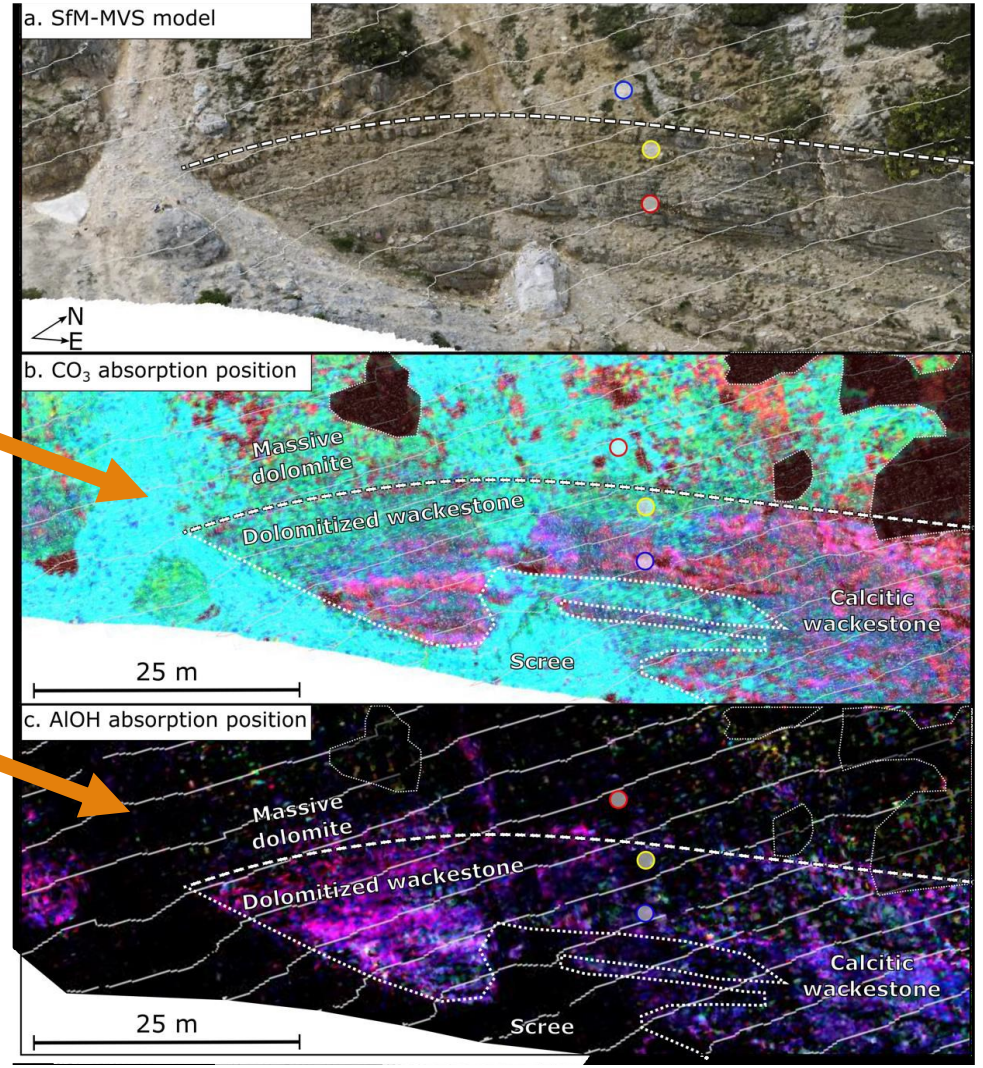

Once correction is carried out, an hyperspectral cloud can be generated that carries all the spectral information collected by the hyperspectral camera correctly positioned on the VOM

Thiele et al., 2022

Example 2: Hyperspectral imaging

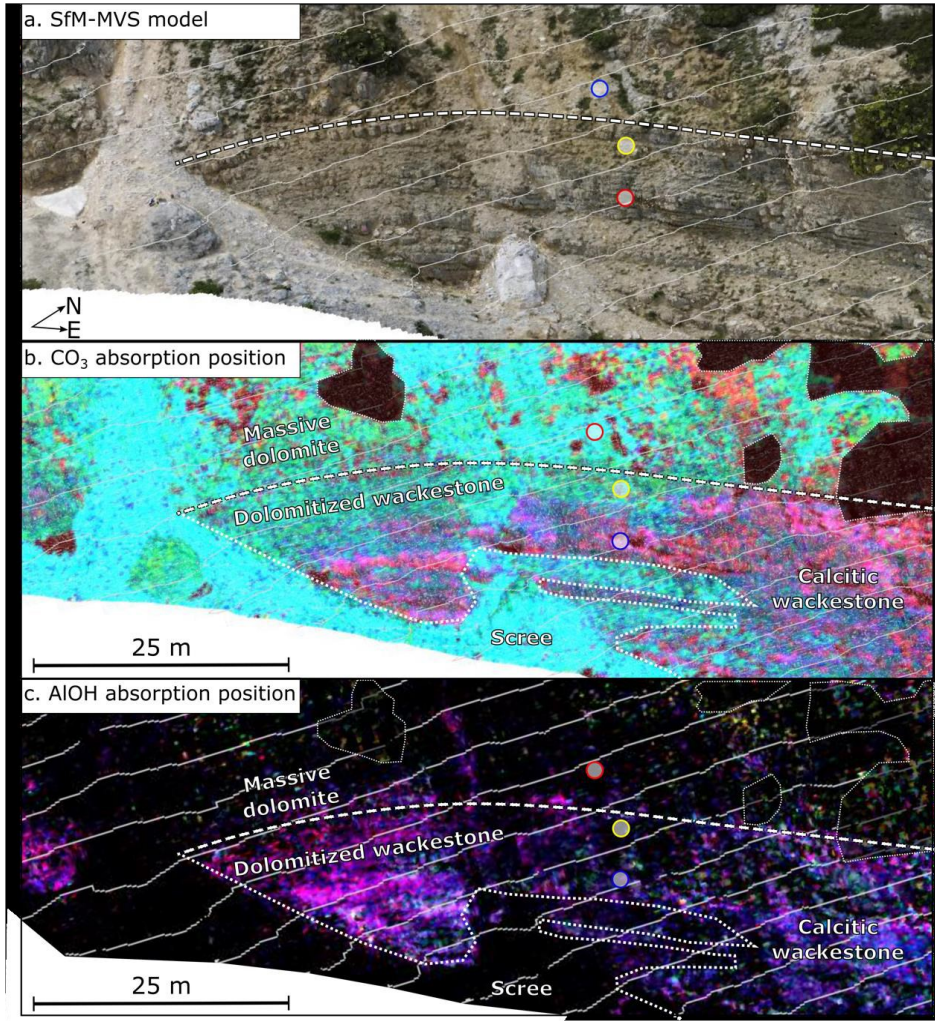

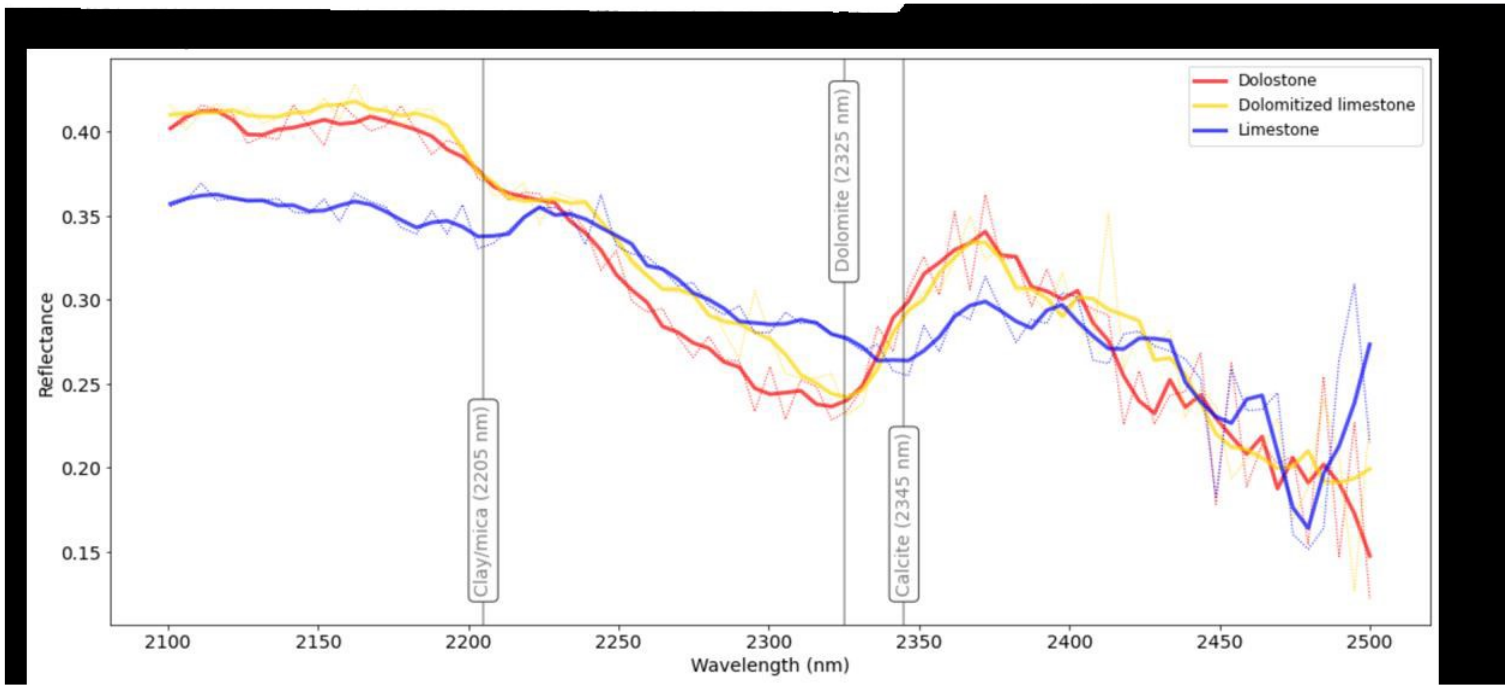

Thiele et al., 2022

Reflectance spectra (above) in three points sampled on the hyperspectral point cloud (left).
The position of absorption bands typical of clay minerals, Dolomite and Calcite are highlighted by grey lines.

Example 3: Facies mapping and analysis.

The Calcare Massiccio formation is made of a thick pile of shallow water carbonates deposited in the Early Jurassic on the Appennine Carbonate Platfrom and extensively outcropping in the Central Apennines

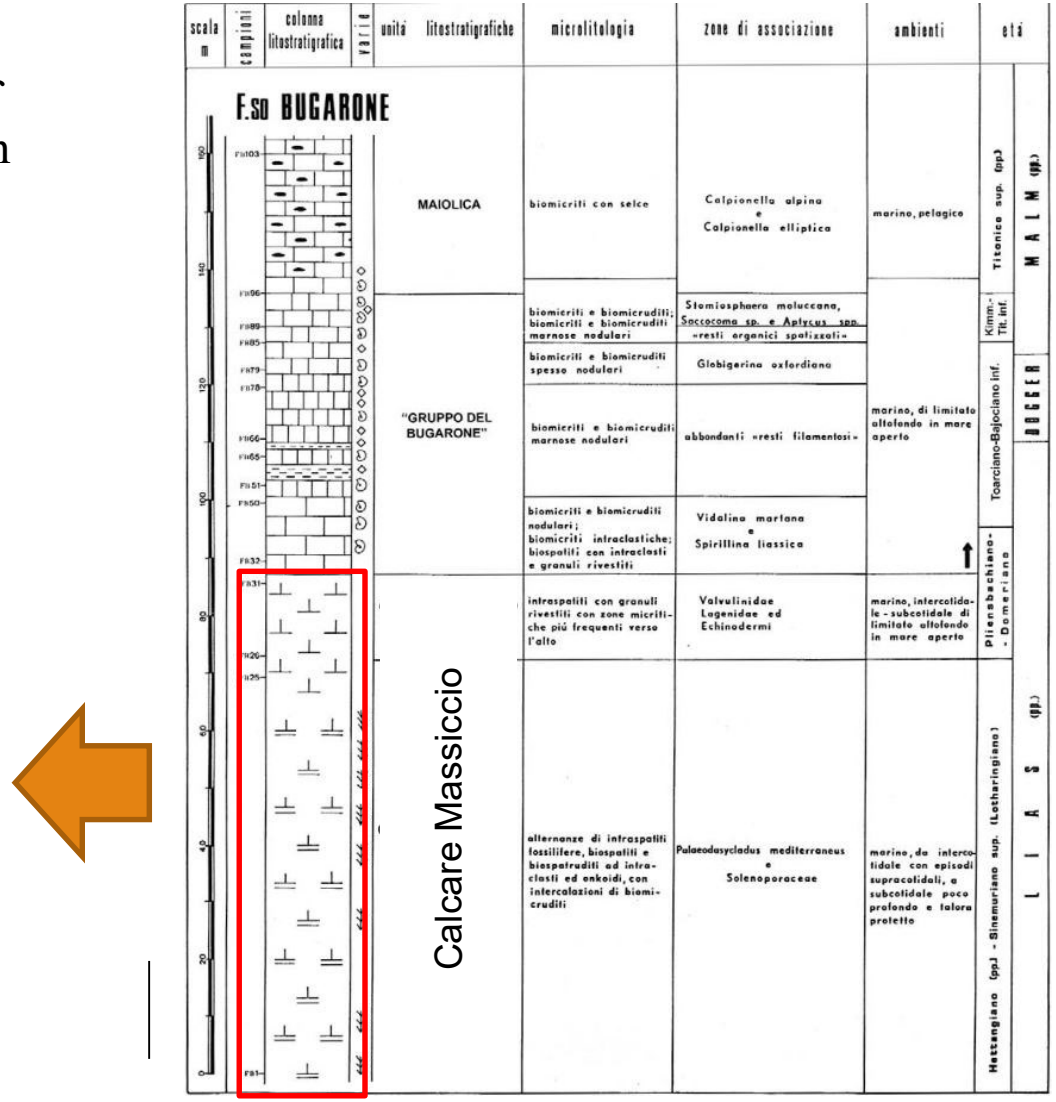

From ISPRA, Quaderno 7

Example 3: Facies mapping and analysis.

The Gola della Rossa quarry (left) near Serra San Quirico (AN), features a spectacular exposure of the Calcare Massiccio.

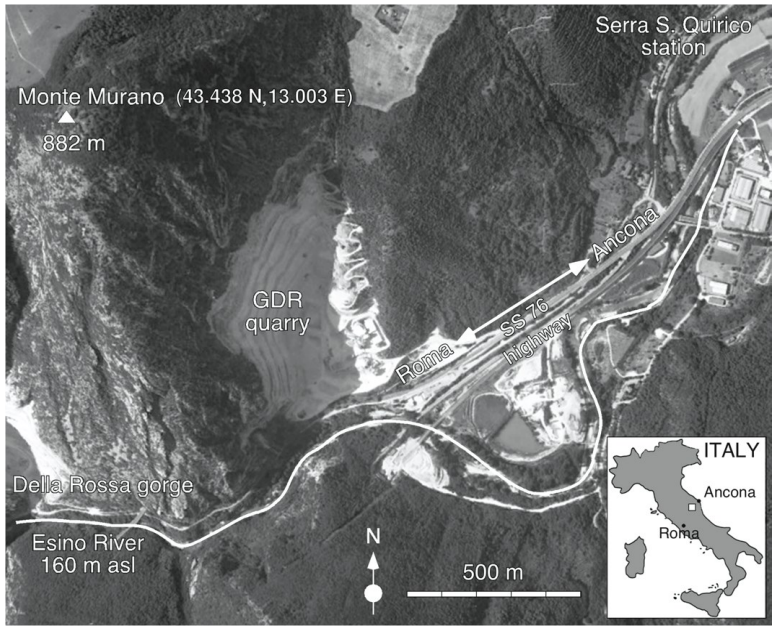

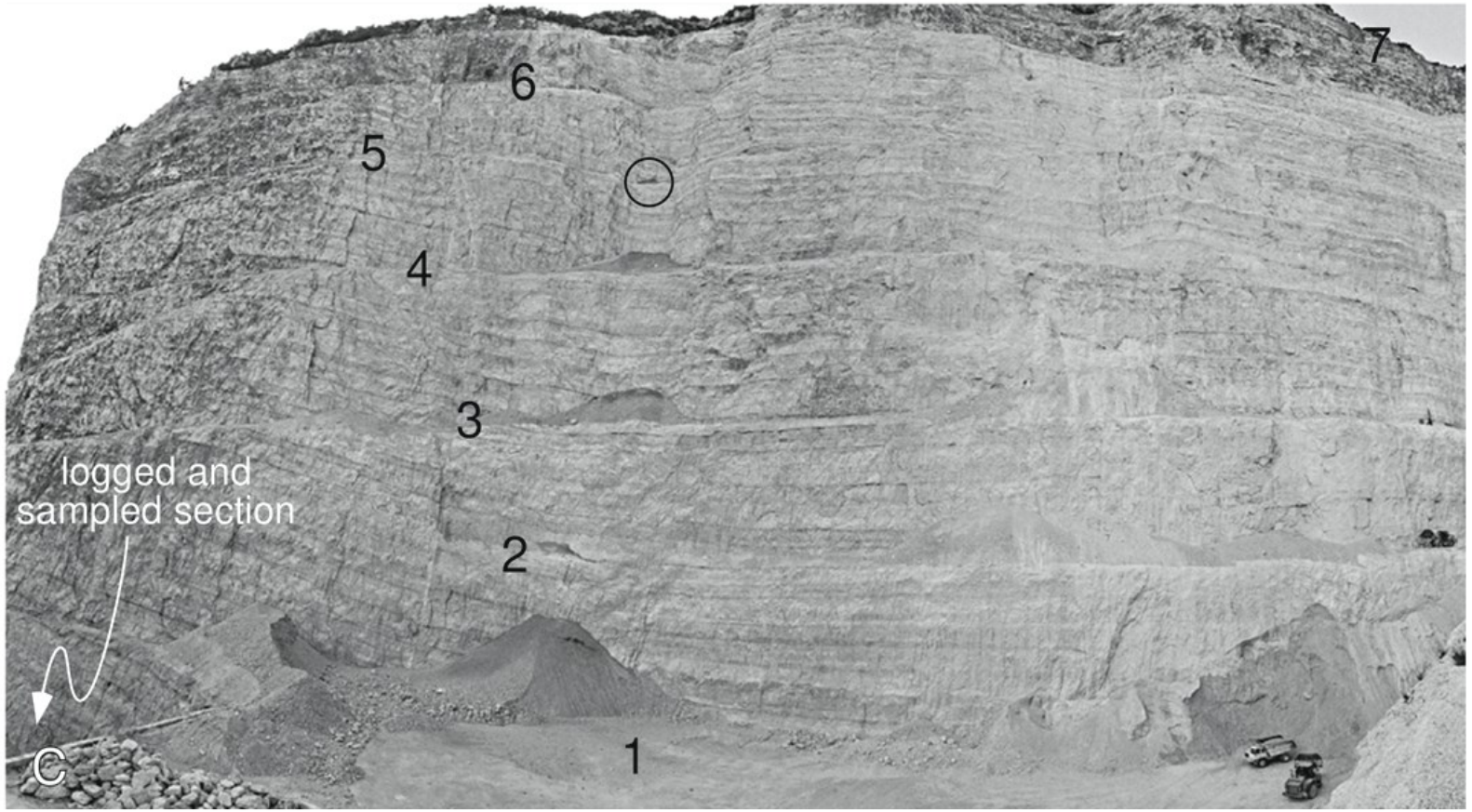

Penasa et al., 2019

The large quarry (see truck in the black circle for scale) and the vertical expsure prevent direct access to the rock in most of the outcrop

Example 3: Facies mapping and analysis.

The lack of biostratigraphically significant fossils makes dating of the Calcare Massiccio particularly difficult.

The succession is strikingly cyclical and made up by hundreds of peritidal cycles.

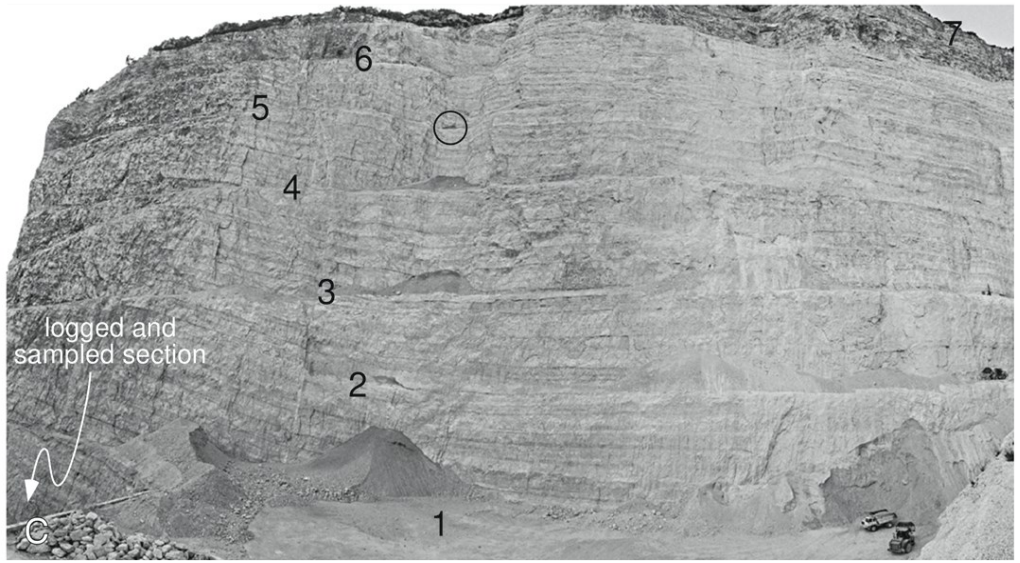

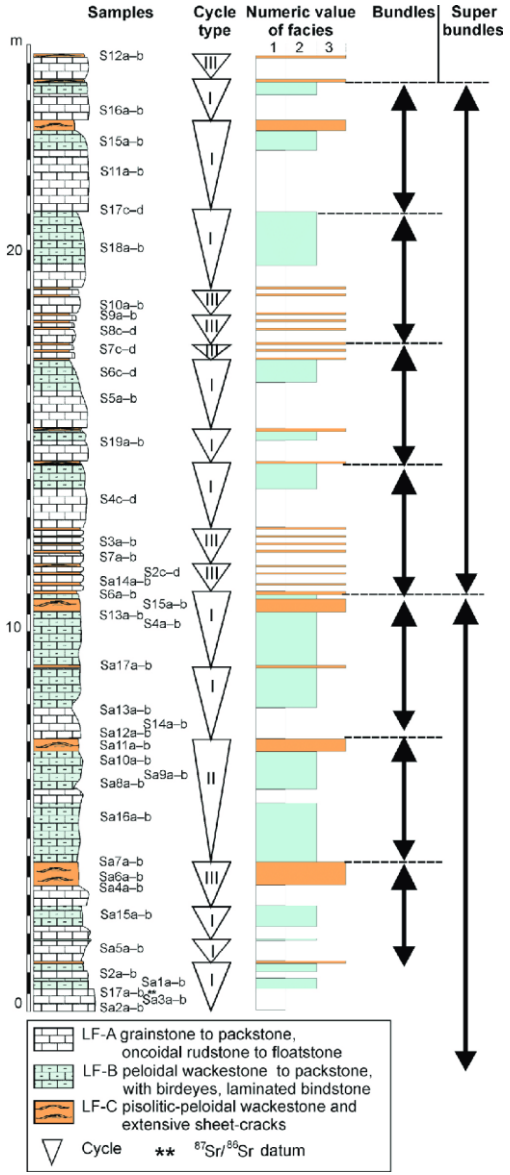

From Brandano et al., 2015

Example 3: Facies mapping and analysis.

A photogrammetric model was built using photos taken from the ground.

On the model, main beds were recognized, traced and correlated in order to identify overlapping regions of interest (ROIs) where the cyclicity was clearly visible.

Photogrammetric VOM

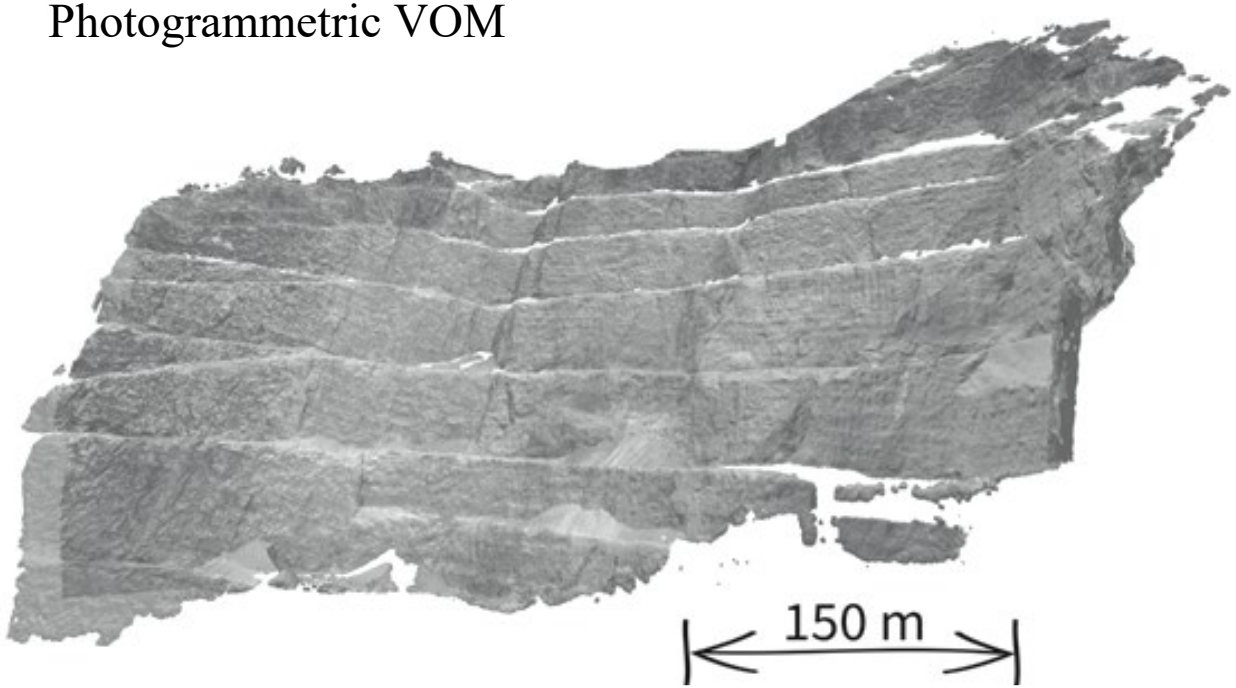

Main beds identified and traced

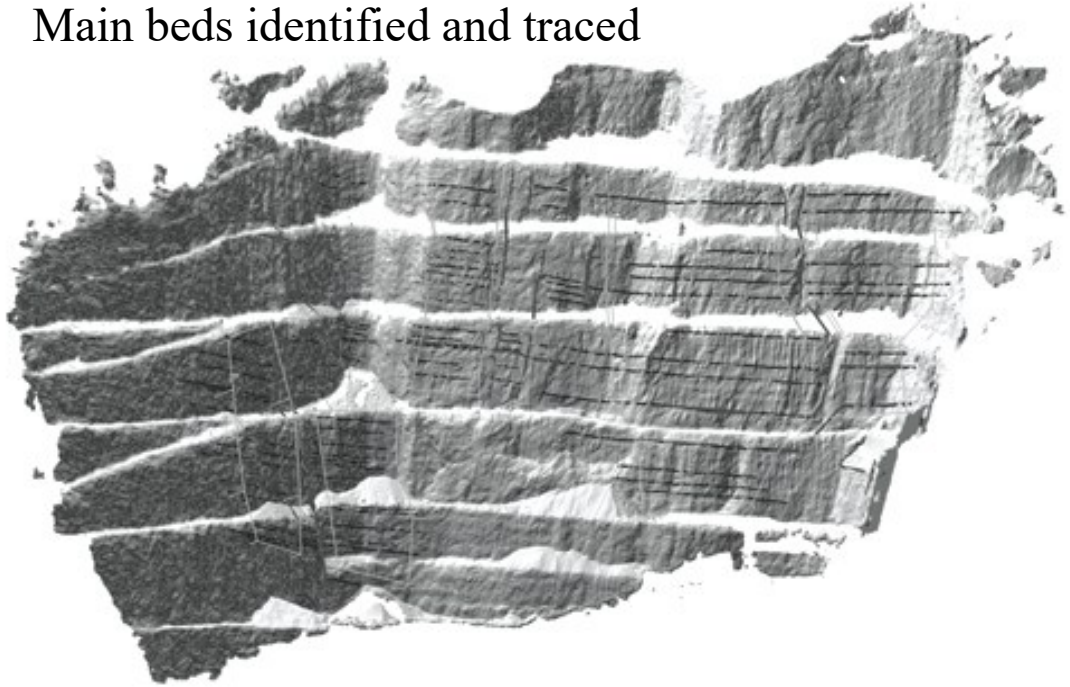

Example 3: Facies mapping and analysis.

From the VOM point cloud with associated RGB texture grayscale logs vere extracted that represent variations of the RGB average channels along the succession.

Direct inspection in an accessible area of the quarry allowed establishing that deeper facies correspond to lighter grayscale colors and shallower facies correspond to shallower water facies.

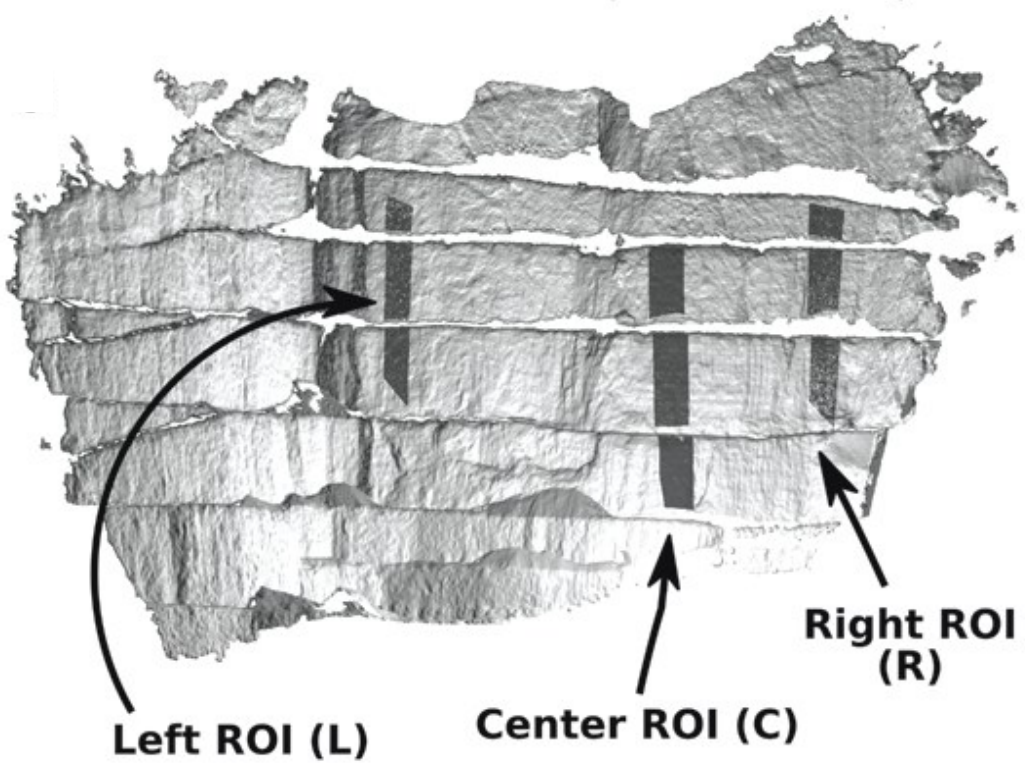

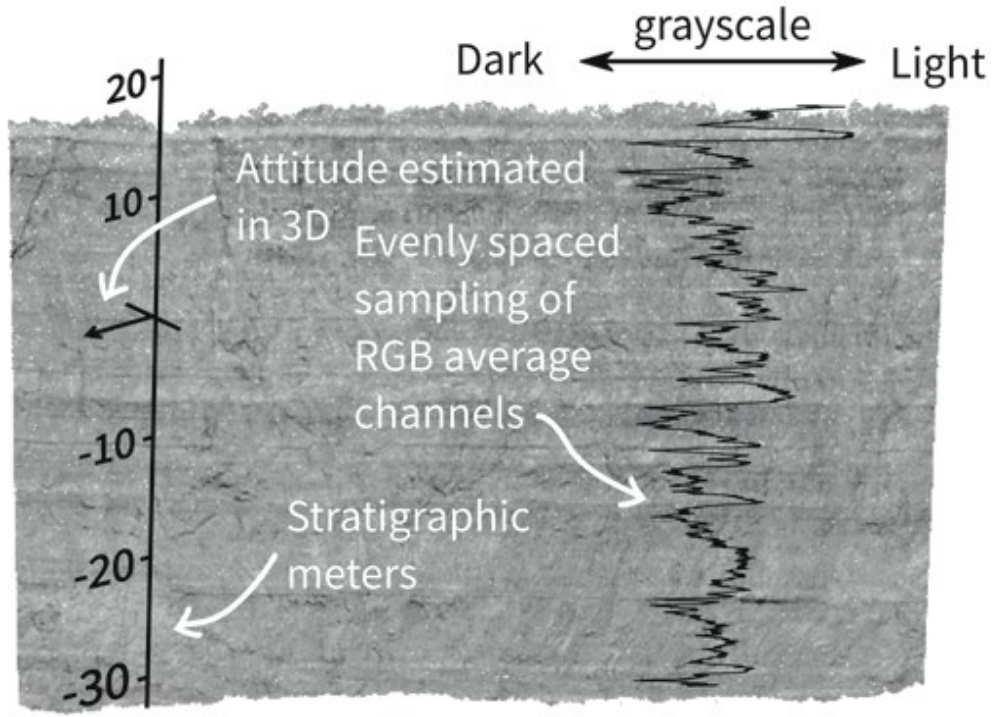

Example 3: Facies mapping and analysis.

On the right, the grayscale log with the color variations can be seen.

The cyclicity is clearly visible and appears organized in larger cyclothems in turn characterized by smaller scale variations in grayscale values.

Such grayscale log, being correctly oriented in the stratigraphic space, is also a time series and therefore can be analyzed using time series analysis methods.

Power spectrum of the greyscale time series.

Peaks exceeding 99% confidence levels are labeled

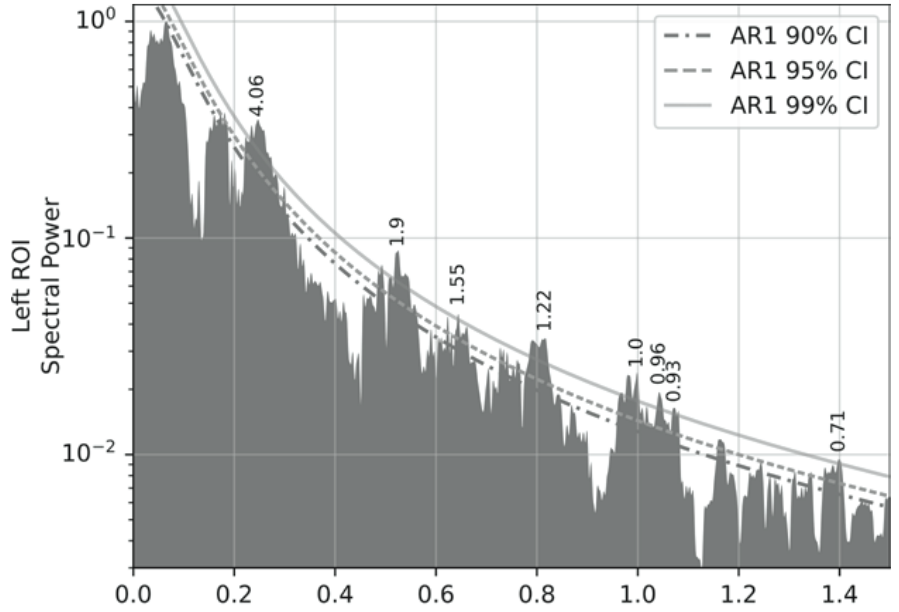

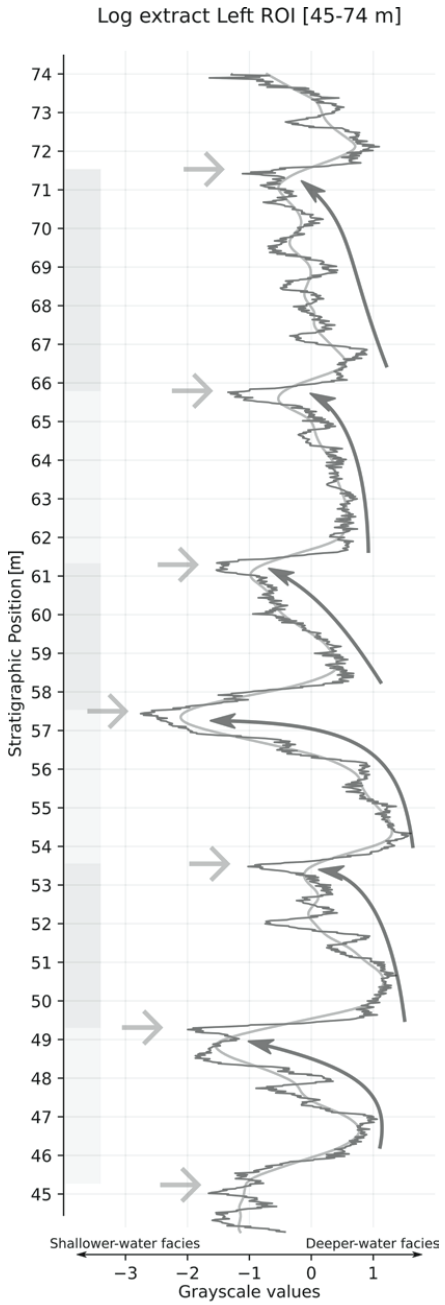

Example 3: Facies mapping and analysis.

Time series analyses reveals that spectral power is concentrated in 5 frequencies bands.

Independent estimation of the sedimentation rate of the average sedimentation rate in the Calcare Massiccio (Brandano et al., 2015) is 5 cm/kyr.

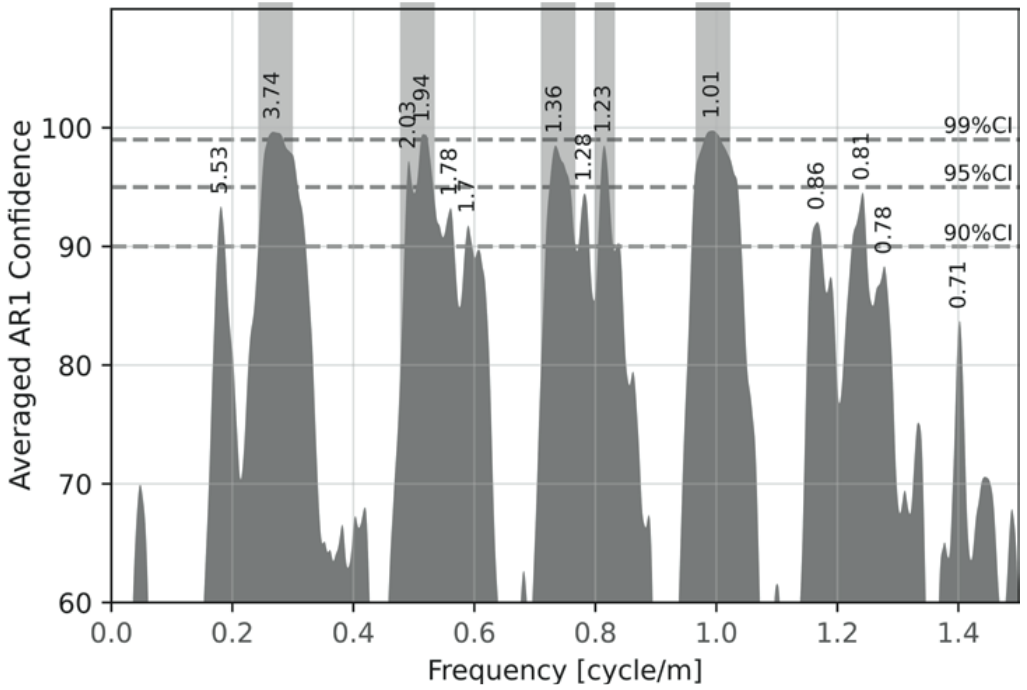

Frequencies in the space domain

5 cm/kyr sed-rate assigned

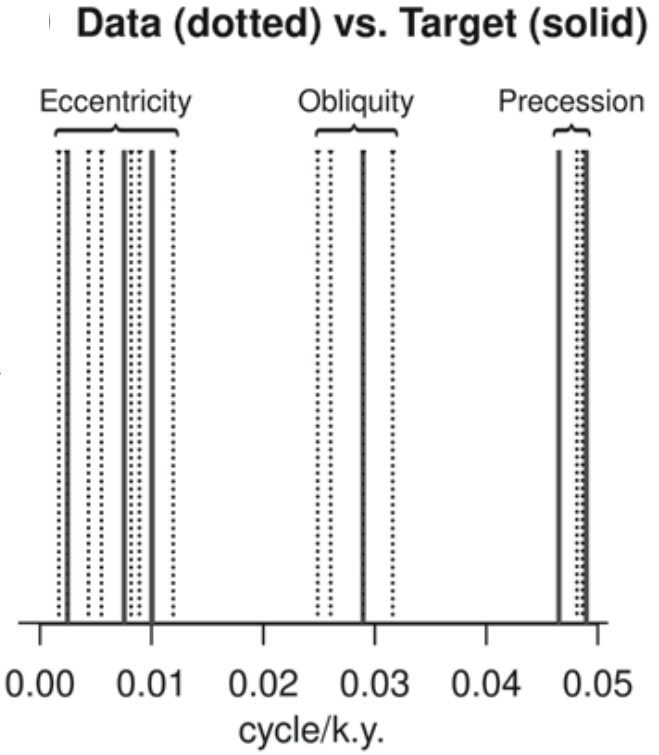

Frequencies in the time domain

Example 4: terrestrial laser scanning intensity analysis

The Scaglia Rossa is a pelagic unit typical that is found in many stratigraphic contexts both in the Sothern Alps and in the Apennines.

The age of the Scaglia Rossa ranges from the Cretaceous to the Eocene.

To the right, an abandoned quarry near Cagli (Umbria Marche Basin) exposing Scaglia Rossa which here is Eocene in age.

Franceschi et al., 2015

Example 4: terrestrial laser scanning intensity analysis

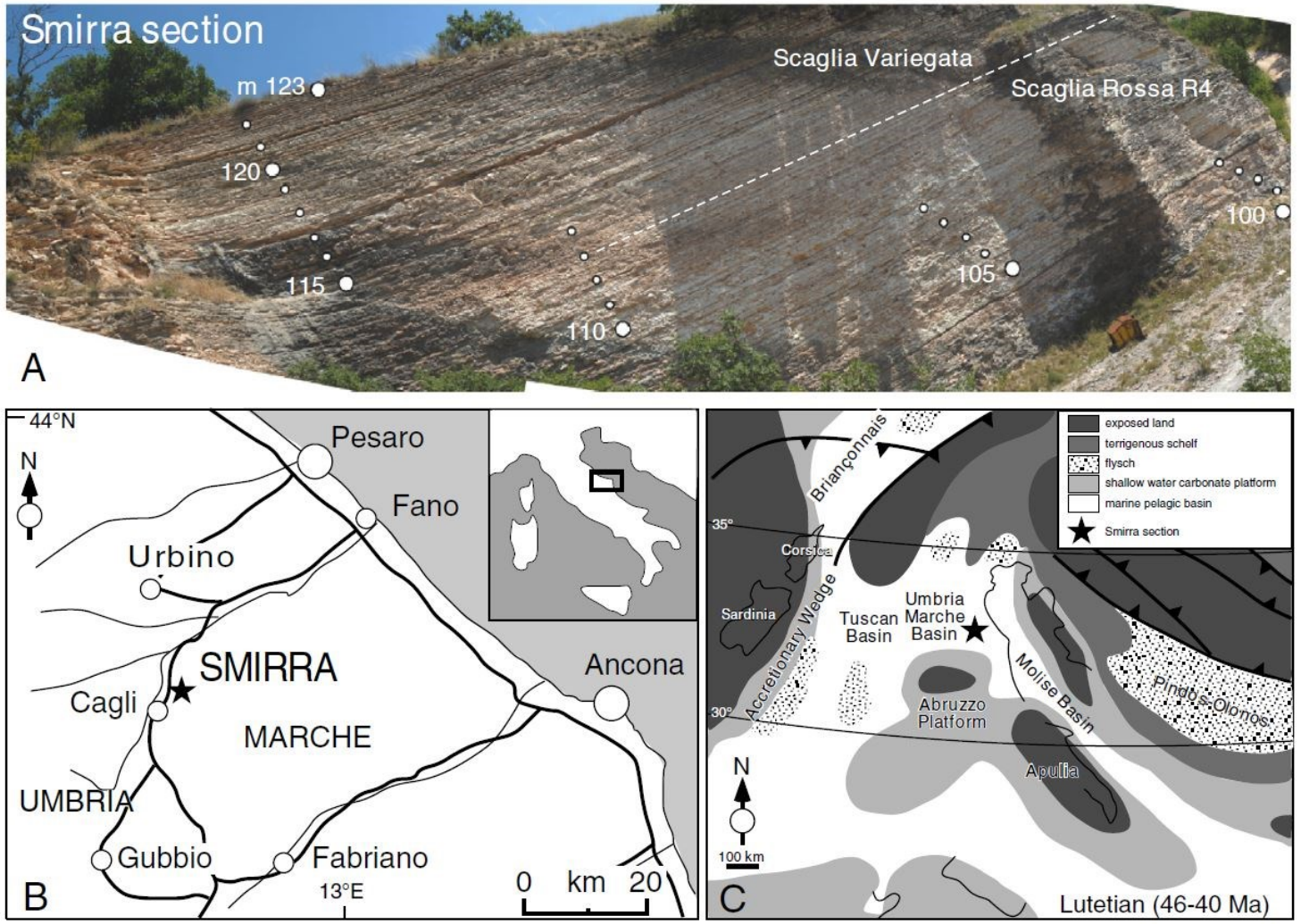

Franceschi et al., 2015

Example 4: terrestrial laser scanning intensity analysis

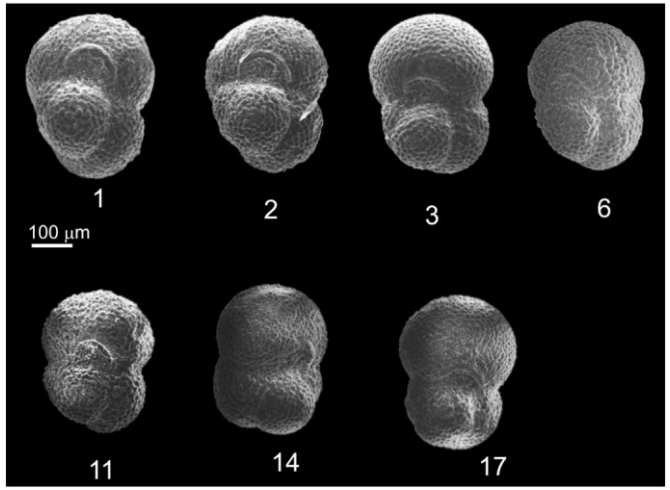

Biostratigraphic investigations and magnetostratigraphy

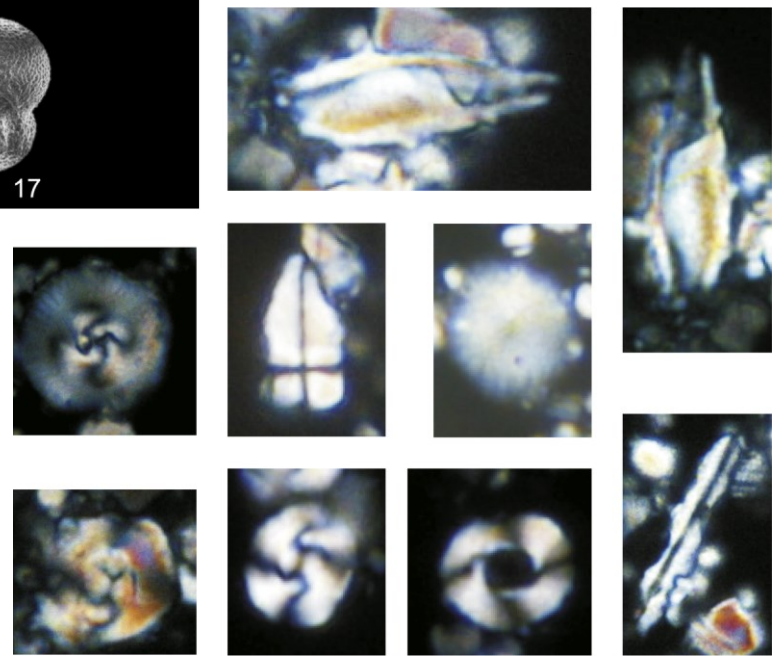

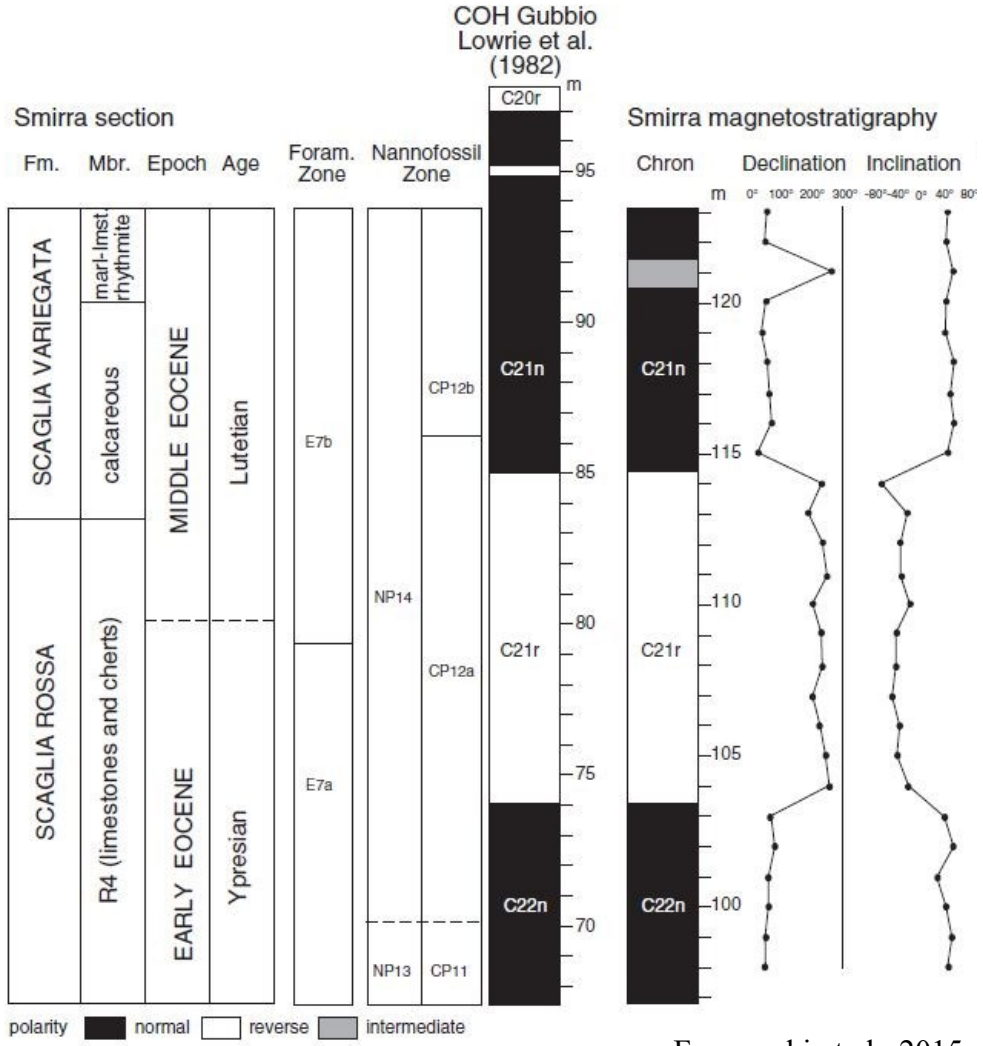

Franceschi et al., 2015

Example 4: terrestrial laser scanning intensity analysis

Construction of intensity series

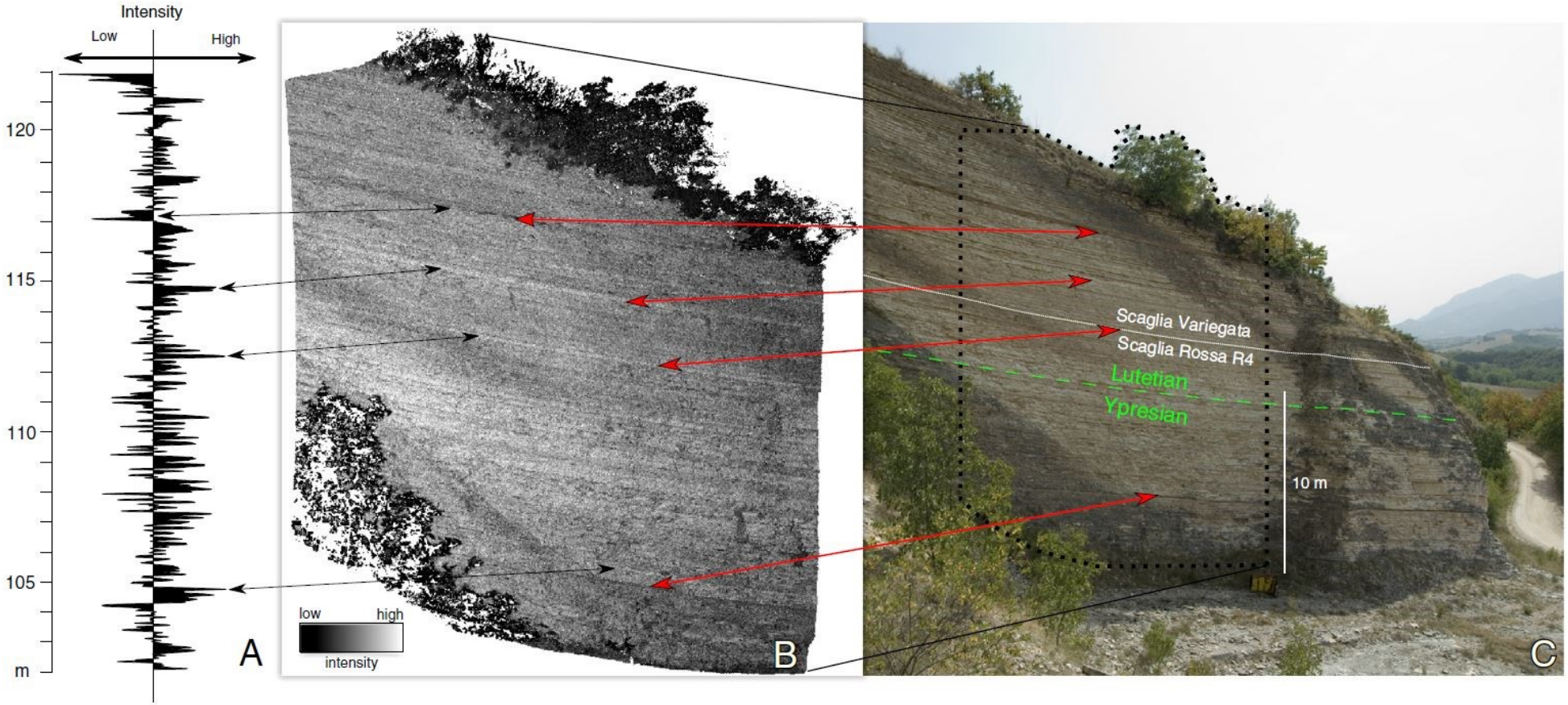

Franceschi et al., 2015

TLS intensity depends on the reflectance of the surface with respect to the laser beam. Reflectance is also determined by the lithological characteristics of the rock

Example 4: terrestrial laser scanning intensity analysis

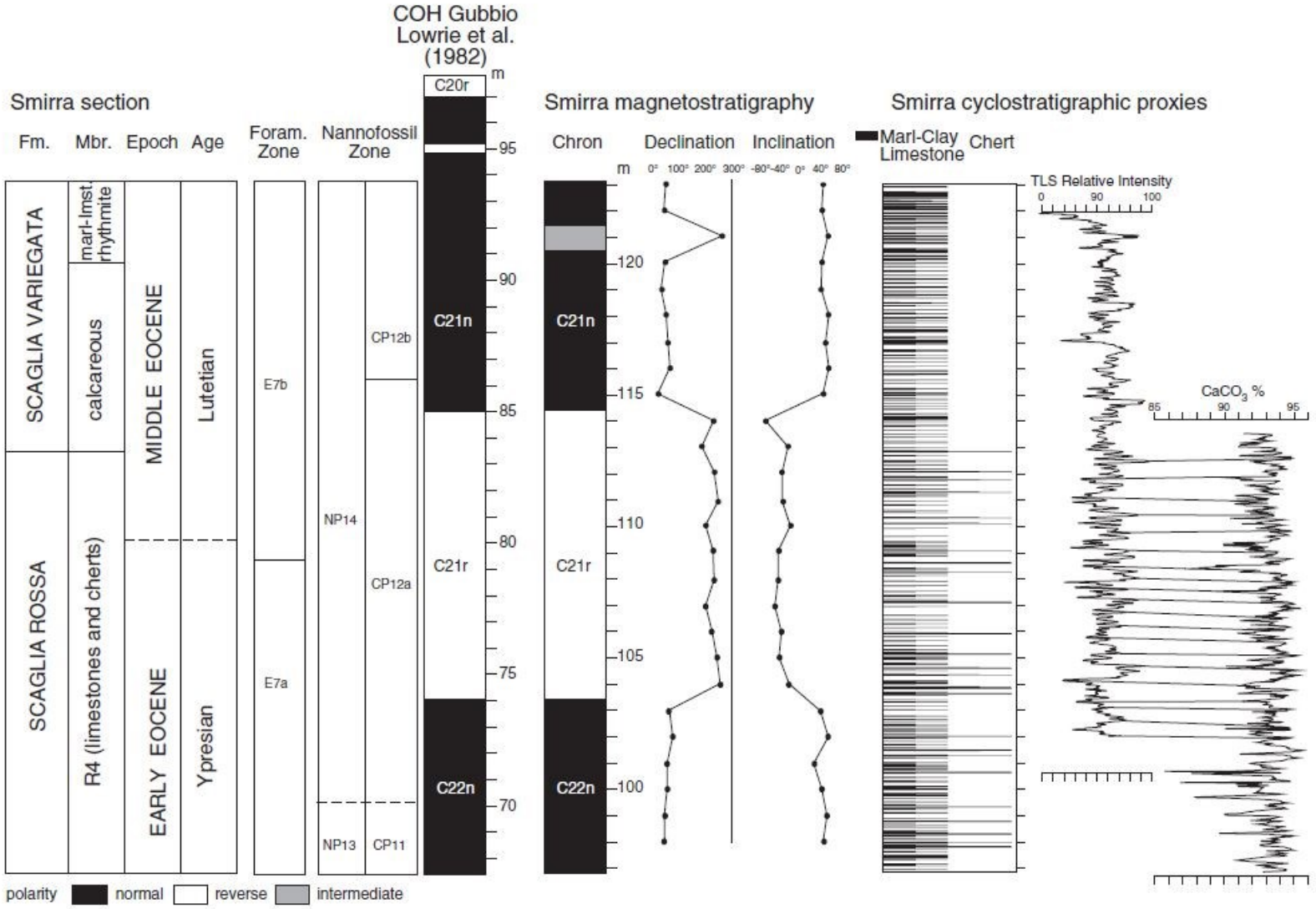

Franceschi et al., 2015

Example 4: terrestrial laser scanning intensity analysis

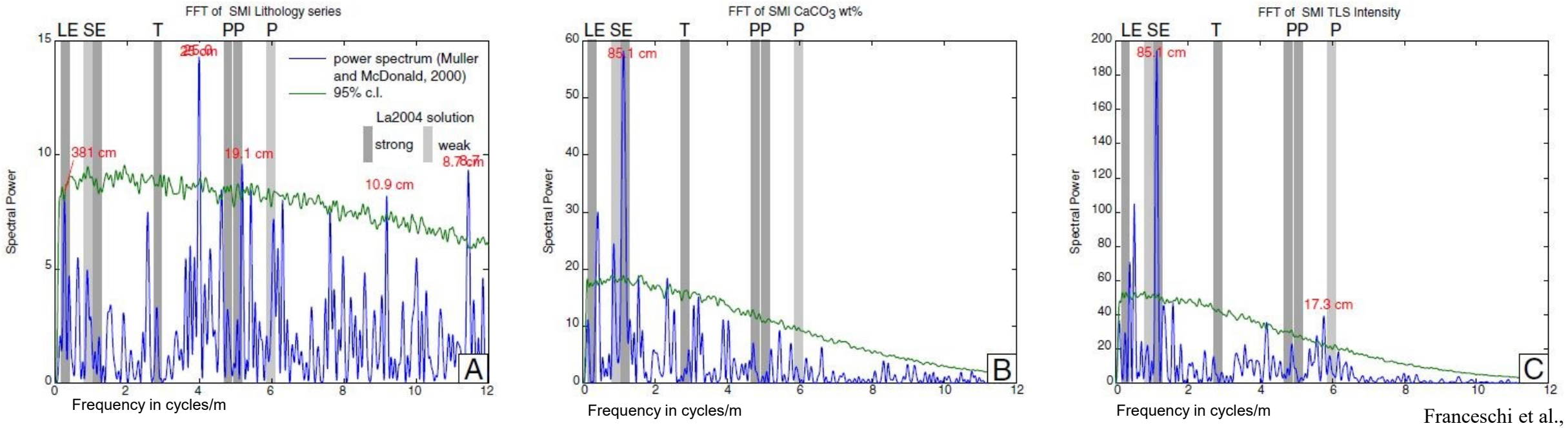

Franceschi et al., 2015

Time series analysis of data extracted from the Smirra outcrop. The TLS intensity derives from the Smirra outcrop virtual outcrop model.

Example 4: terrestrial laser scanning intensity analysis

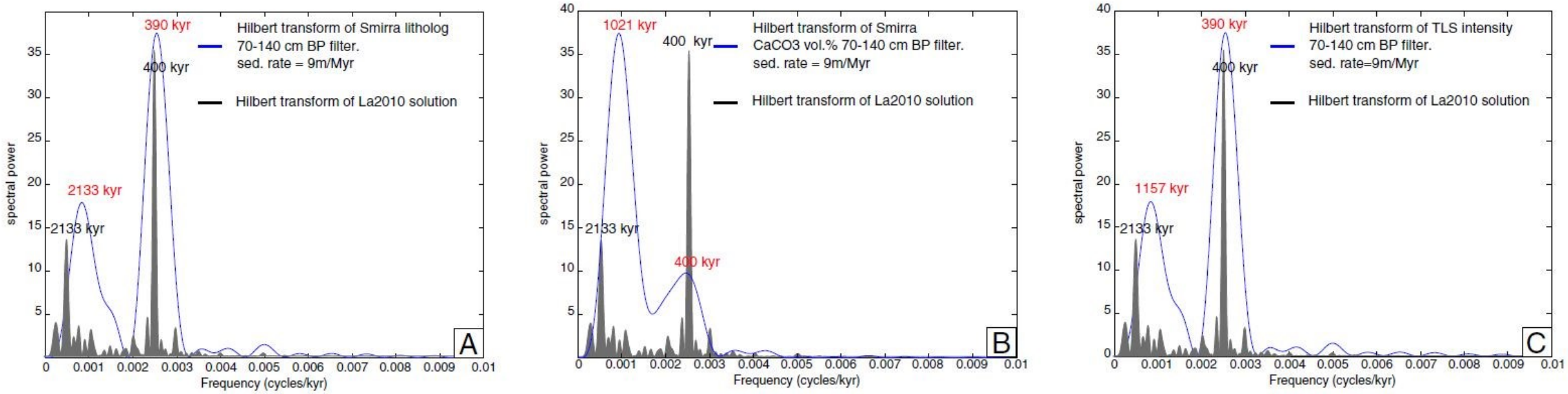

Franceschi et al., 2015

Time series analysis of data extracted from the Smirra outcrop (blue line) expressed in time domain. Passage to the time domain has been obtained assigning the sedimentation rate of 9 mm/Myr estimated by Coccioni et al. (2012). The dark gray spectrum refers to the La2021 astronomical solution for the Eocene.

Example 5: Comet 67P/Churyumov-Gerasimenko

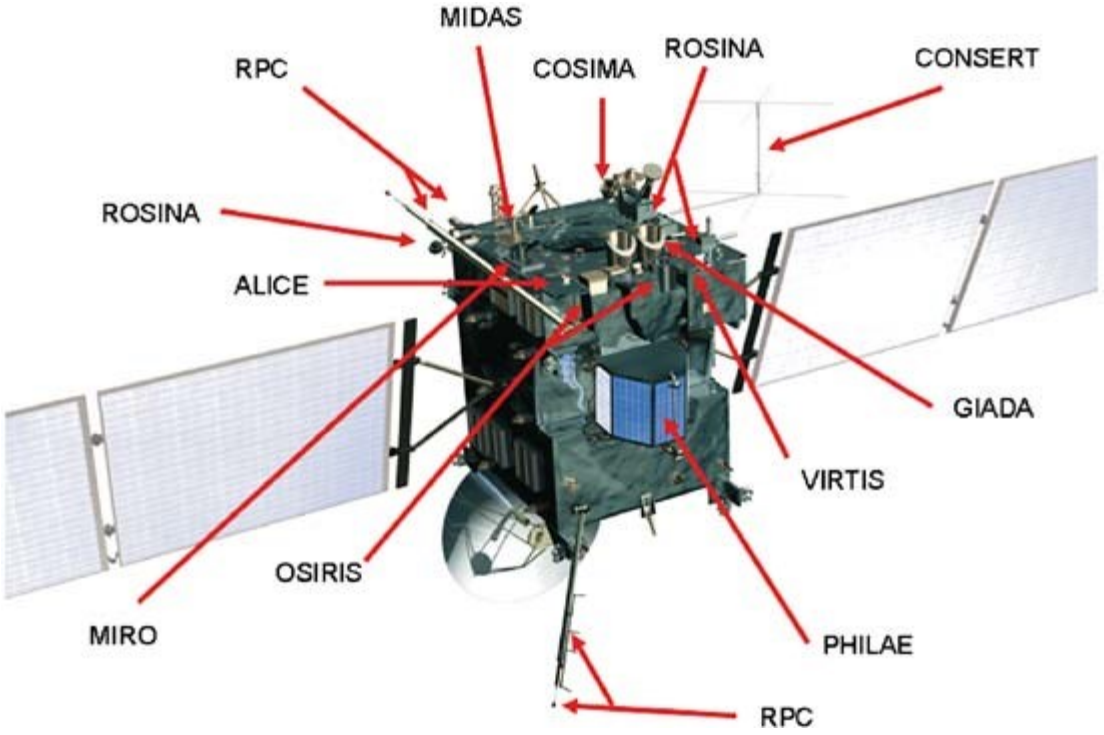

The Rosetta spacecraft

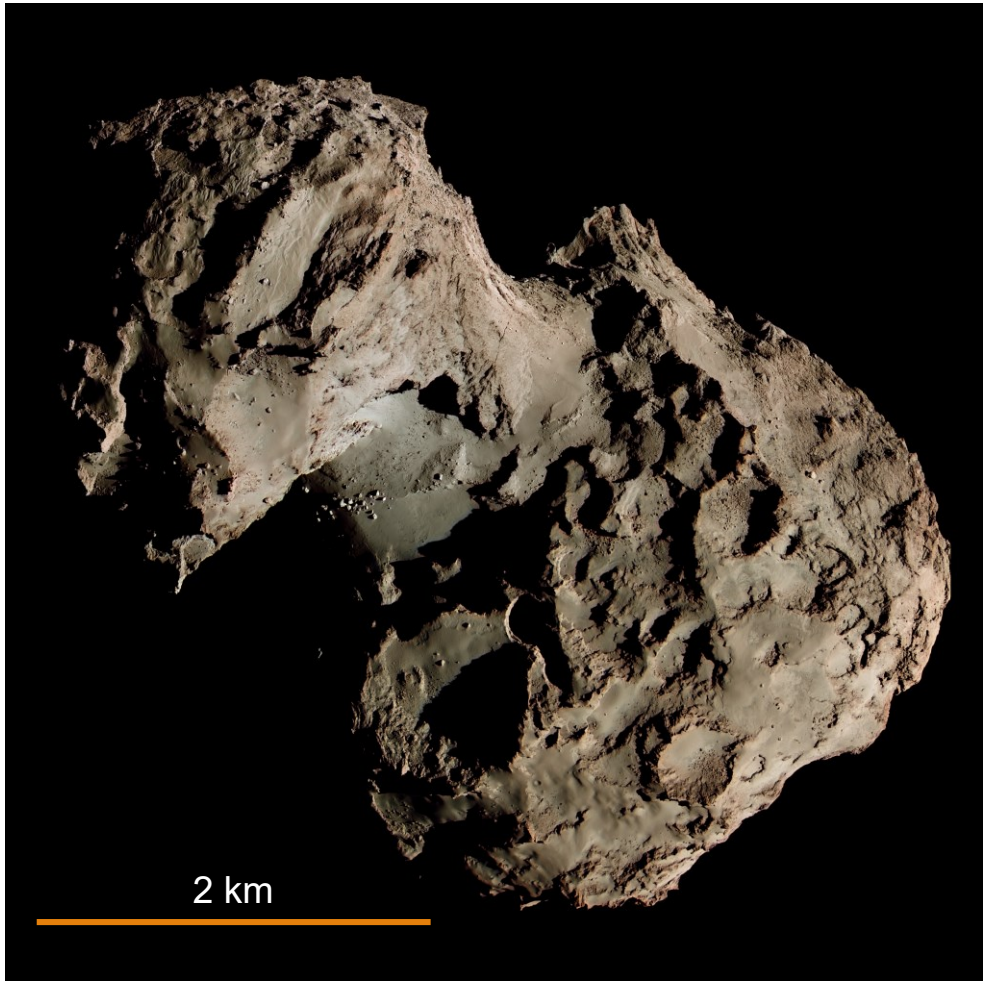

Comet 67P Churyumov-Gerasimenko

Example 5: Comet 67P/Churyumov-Gerasimenko

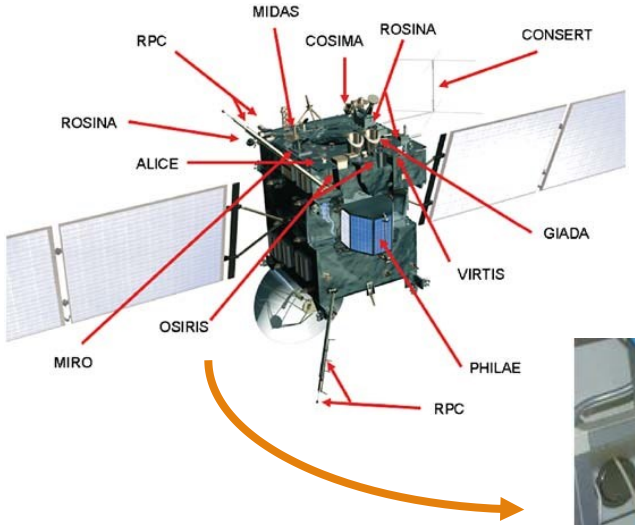

OSIRIS narrow angle camera (NAC)

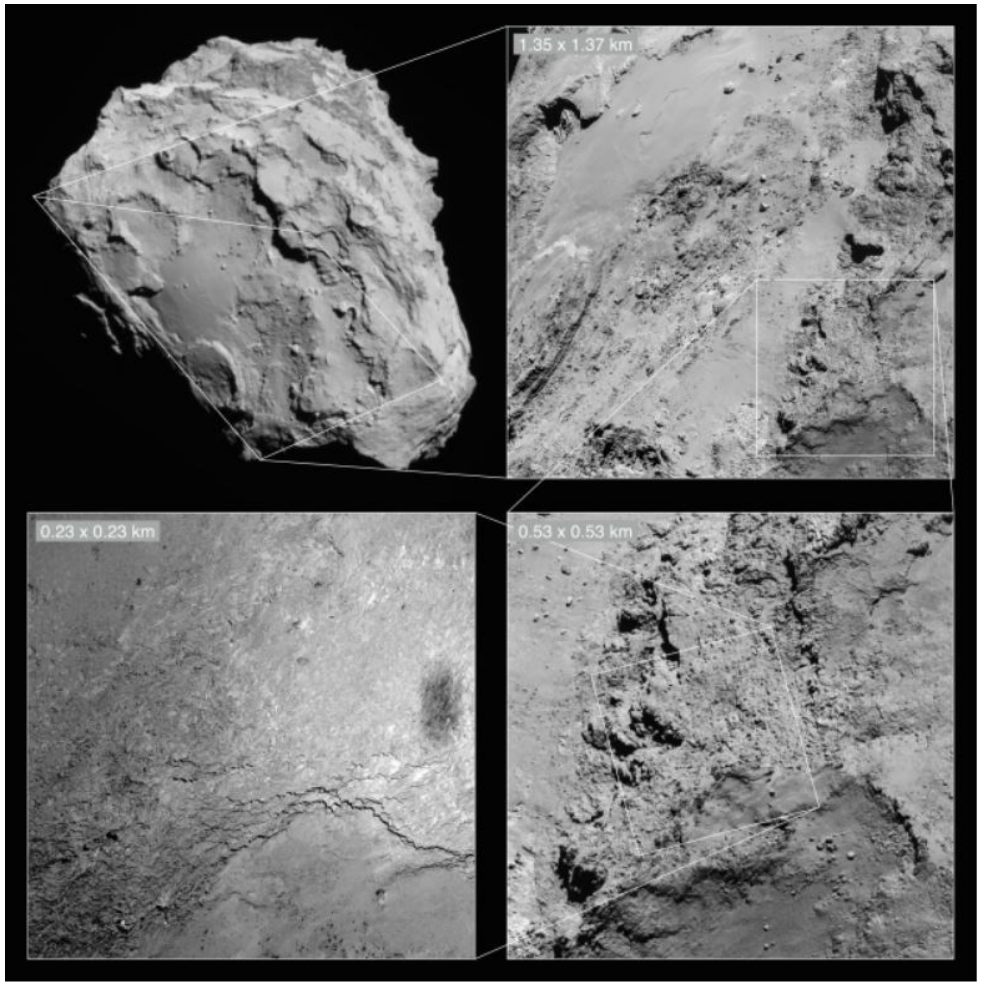

NAC images of 67P surface

Example 5: Comet 67P/Churyumov-Gerasimenko

Stereophotogrammetric analysis

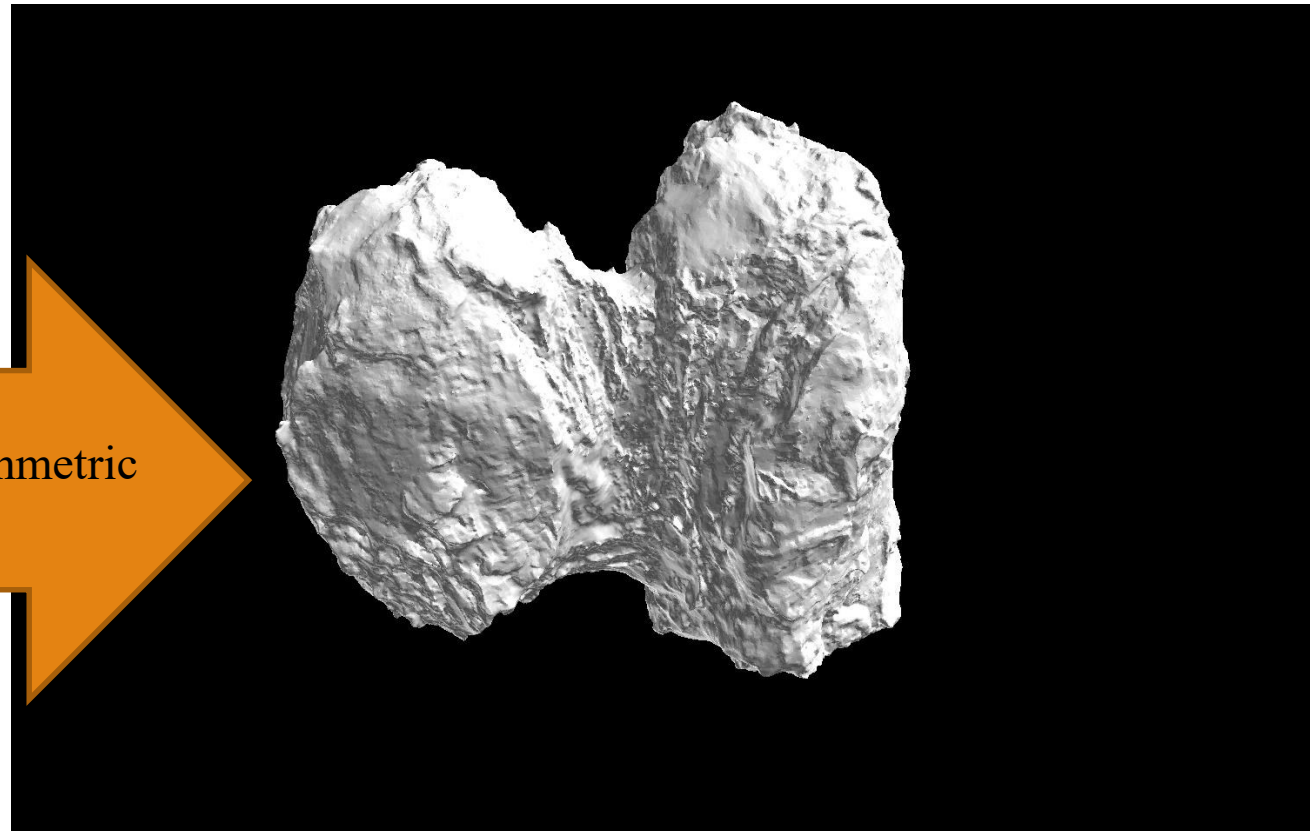

High resolution shape model of comet 67P

Example 5: Comet 67P/Churyumov-Gerasimenko

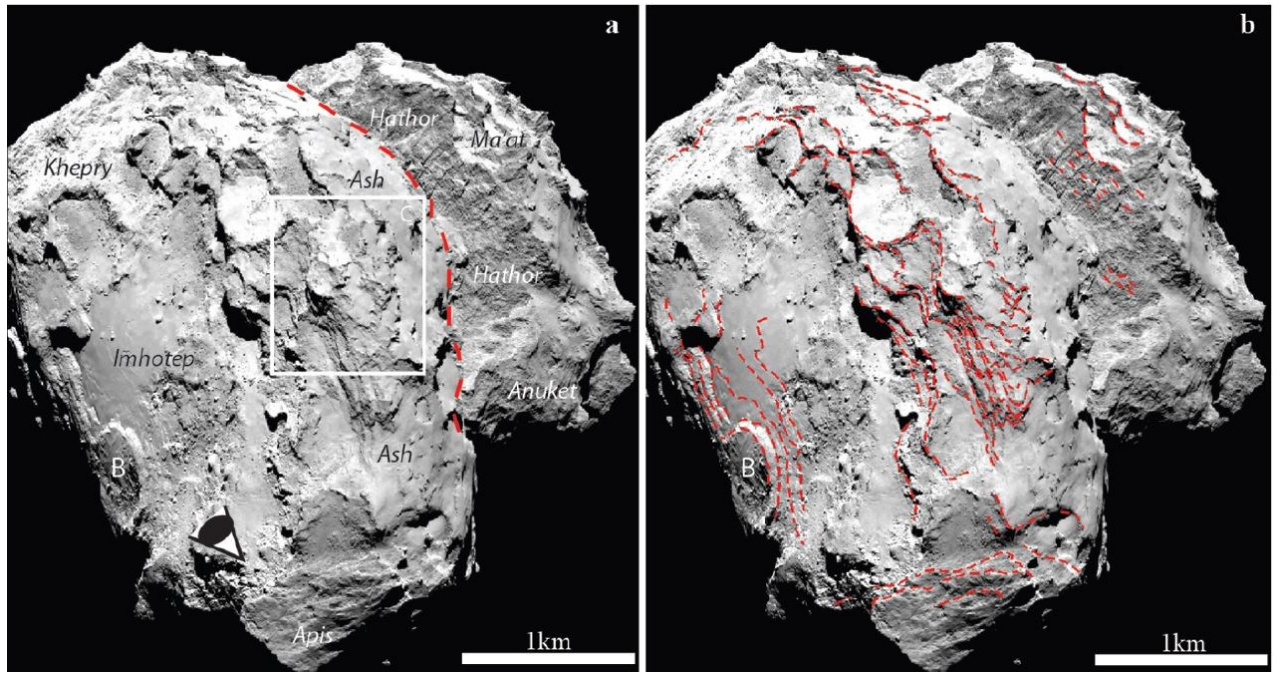

Analysis of the photogrammetric shape model revealed that the comet is layered and the two lobes are characterized by two independent concentric set of layers.

The origin of the layers is still unclear and matter of debate.

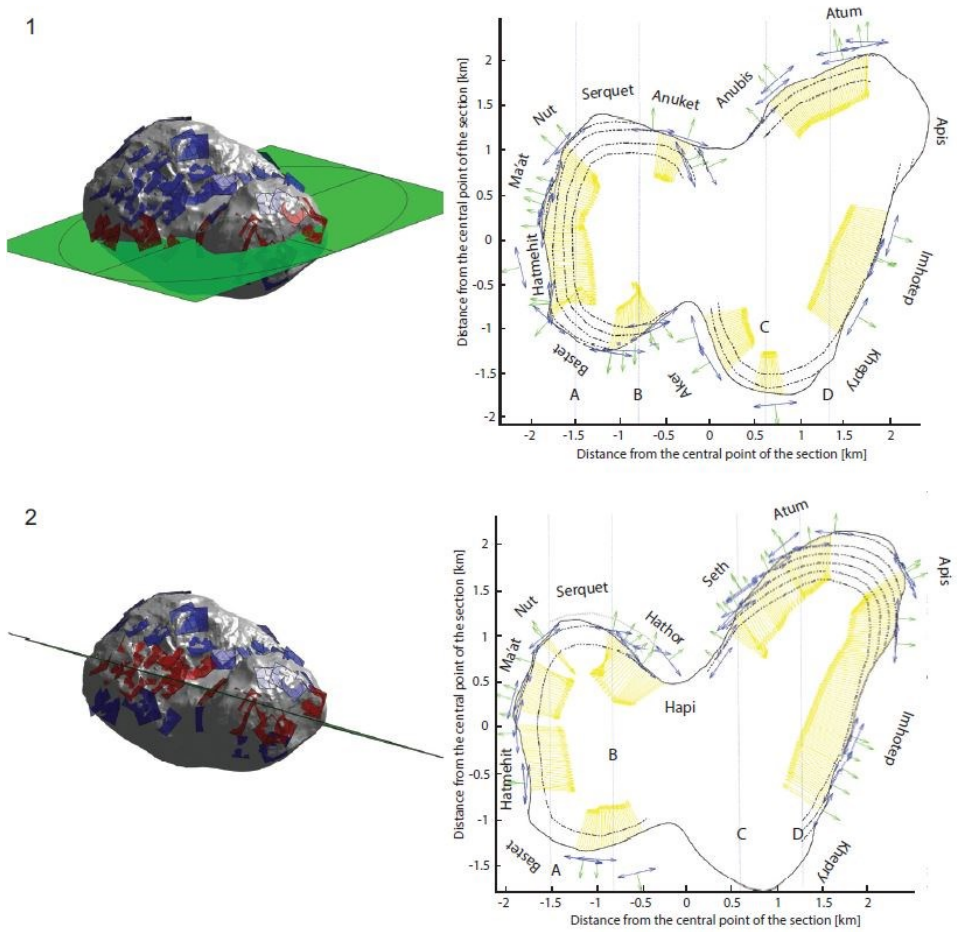

Massironi et al., 2015

Example 5: Comet 67P/Churyumov-Gerasimenko

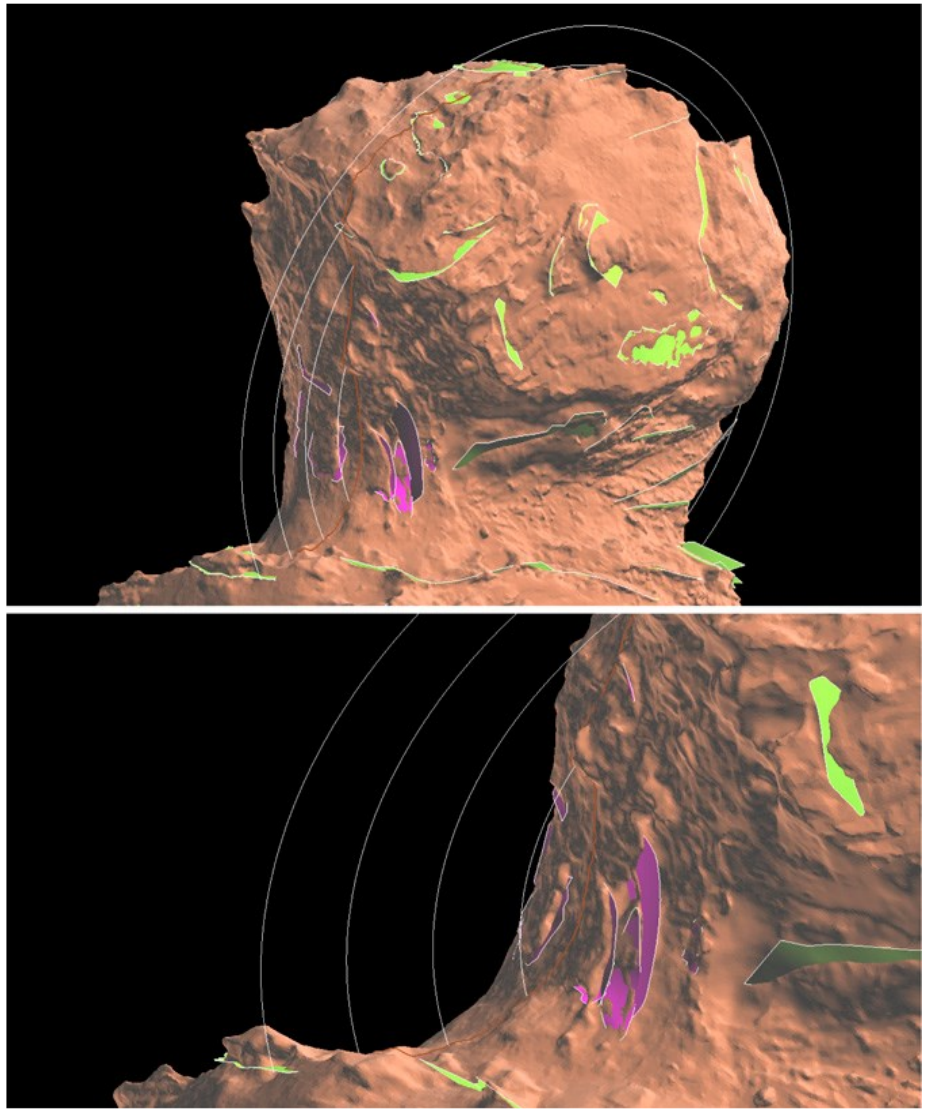

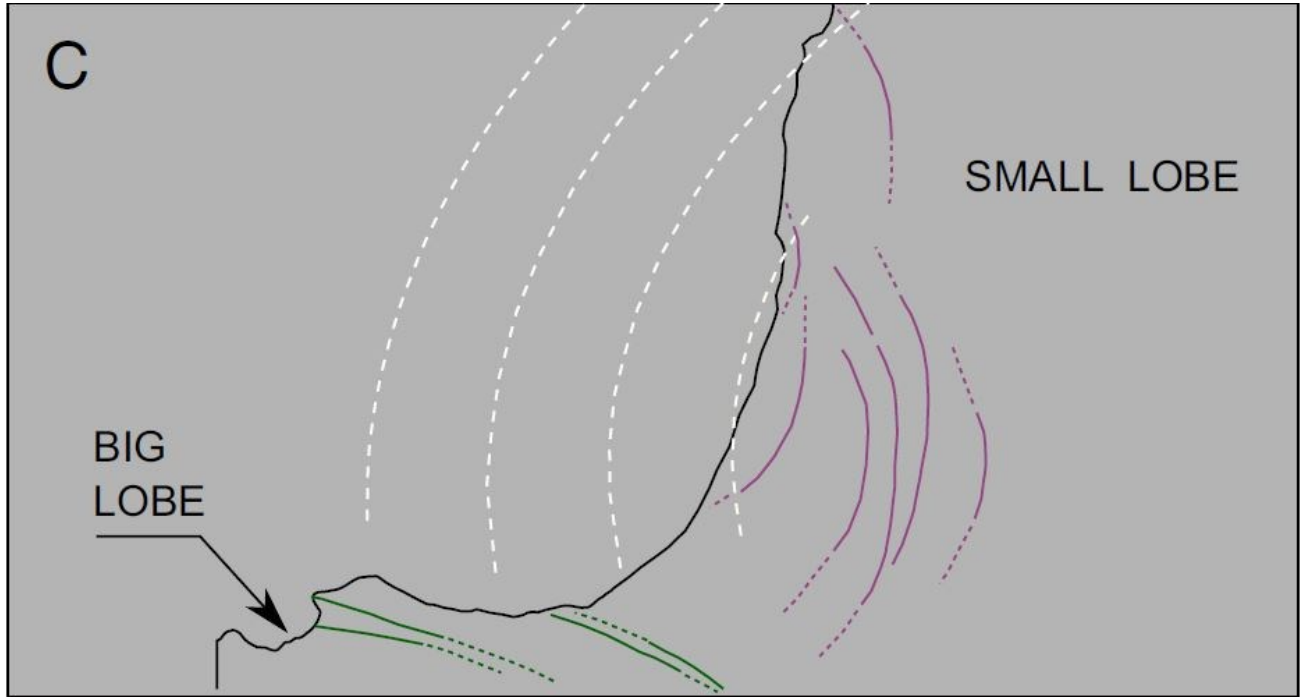

Franceschi et al., 2020

Further observation of the lobe highlighted that nearby the area of junaction of the two lobes there are sectors of the Small Lobe where layers display centre of curvature external to the lobe (i.e. concavity opposite to that expected)

Example 5: Comet 67P/Churyumov-Gerasimenko

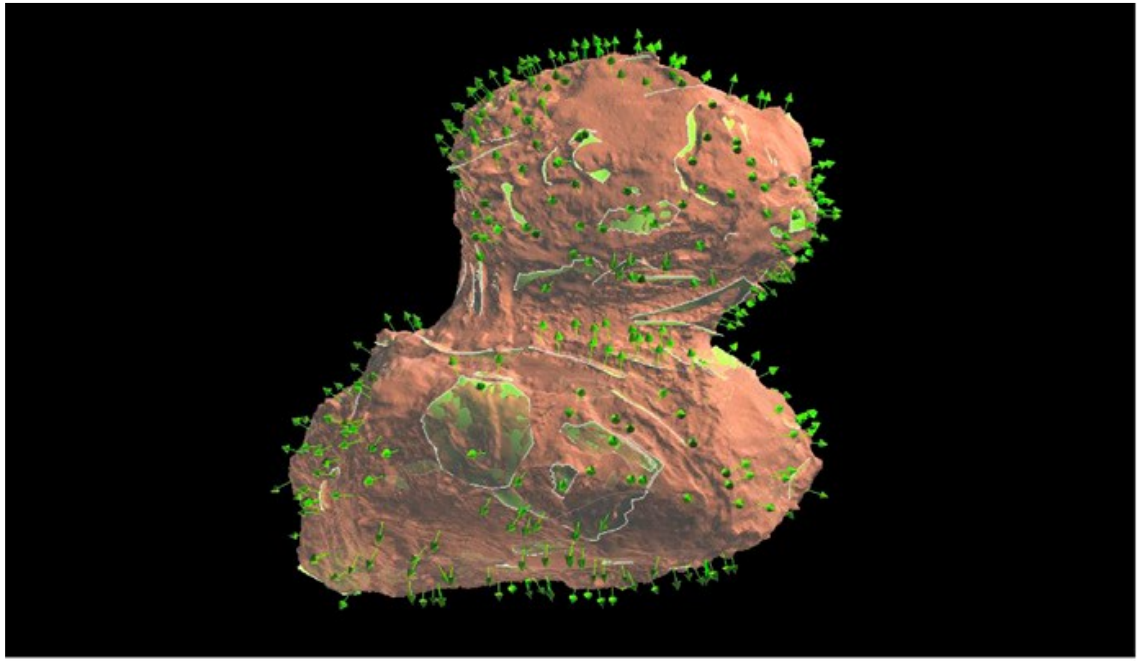

Bedding planes on 67P reconstructed in 3D and normals to bedding planes

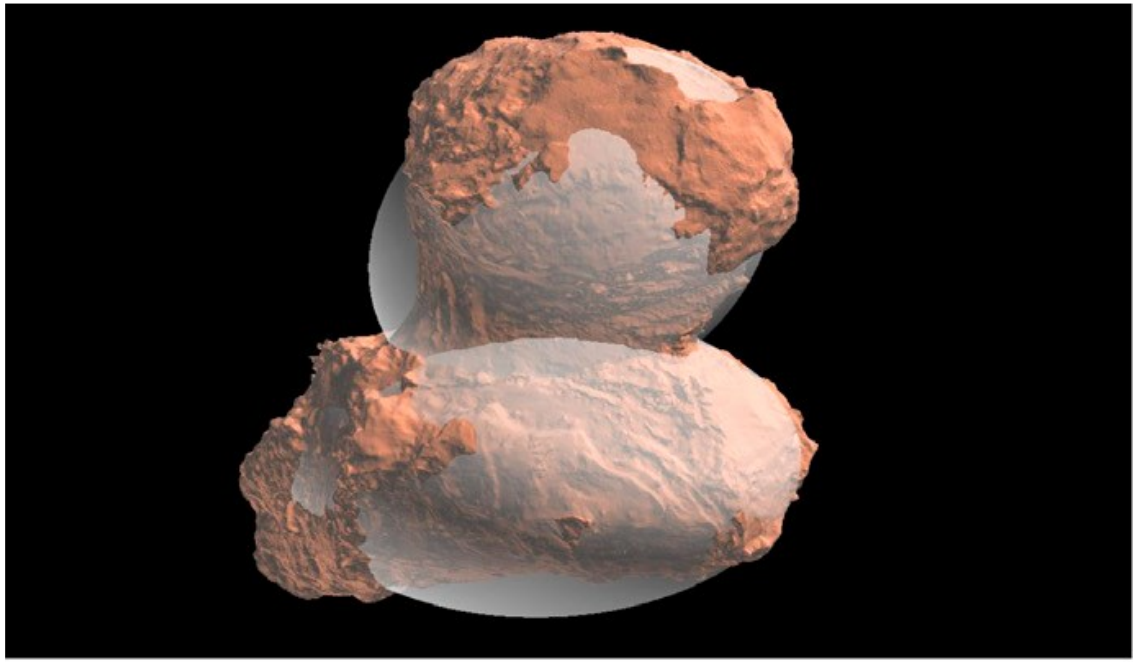

Ellipsoidal models reconstructed by Penasa et al., 2017

Example 5: Comet 67P/Churyumov-Gerasimenko

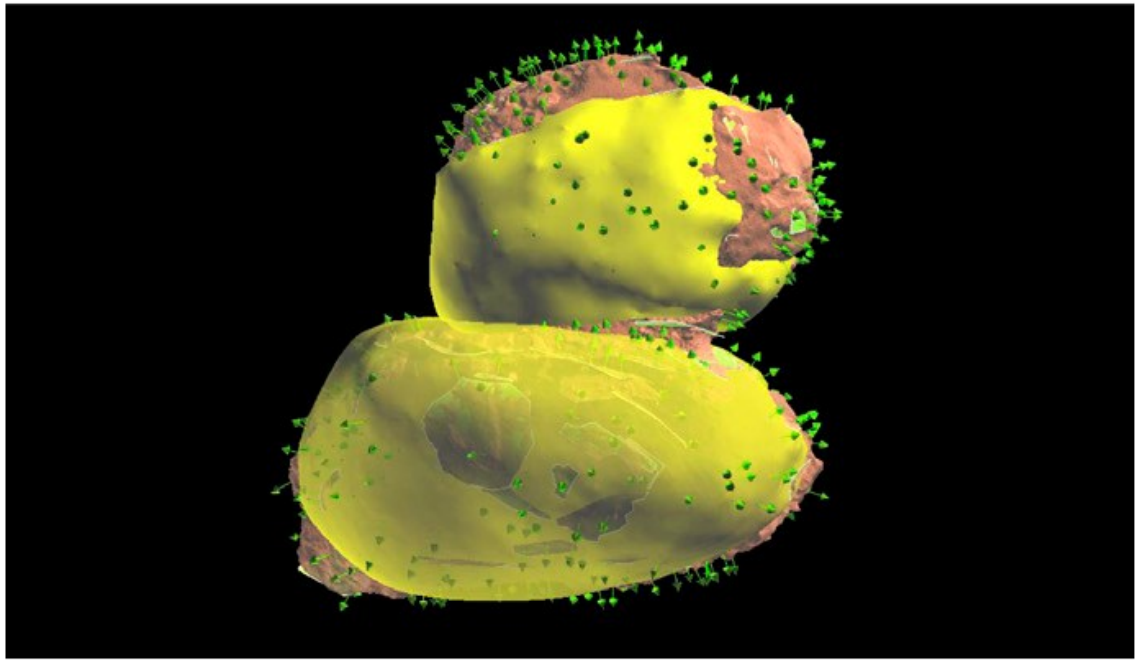

3D model of the layered structure reconstructed using an implicit modeling approach.

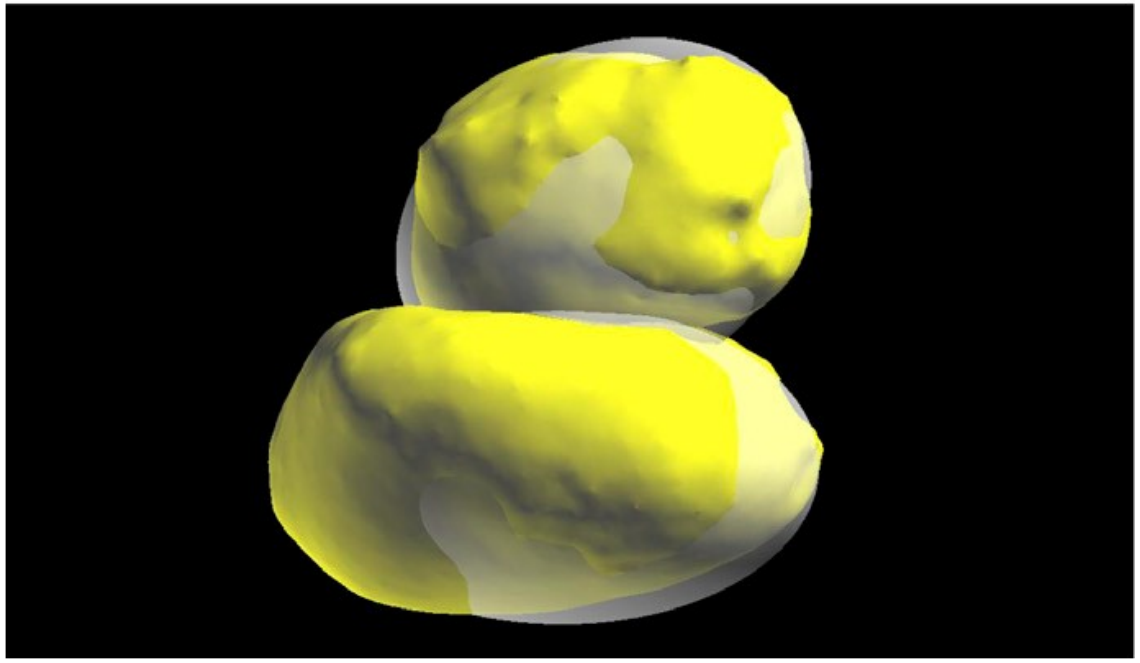

Implicit layerinng model compared to the ellipsoidal models

Example 5: Comet 67P/Churyumov-Gerasimenko

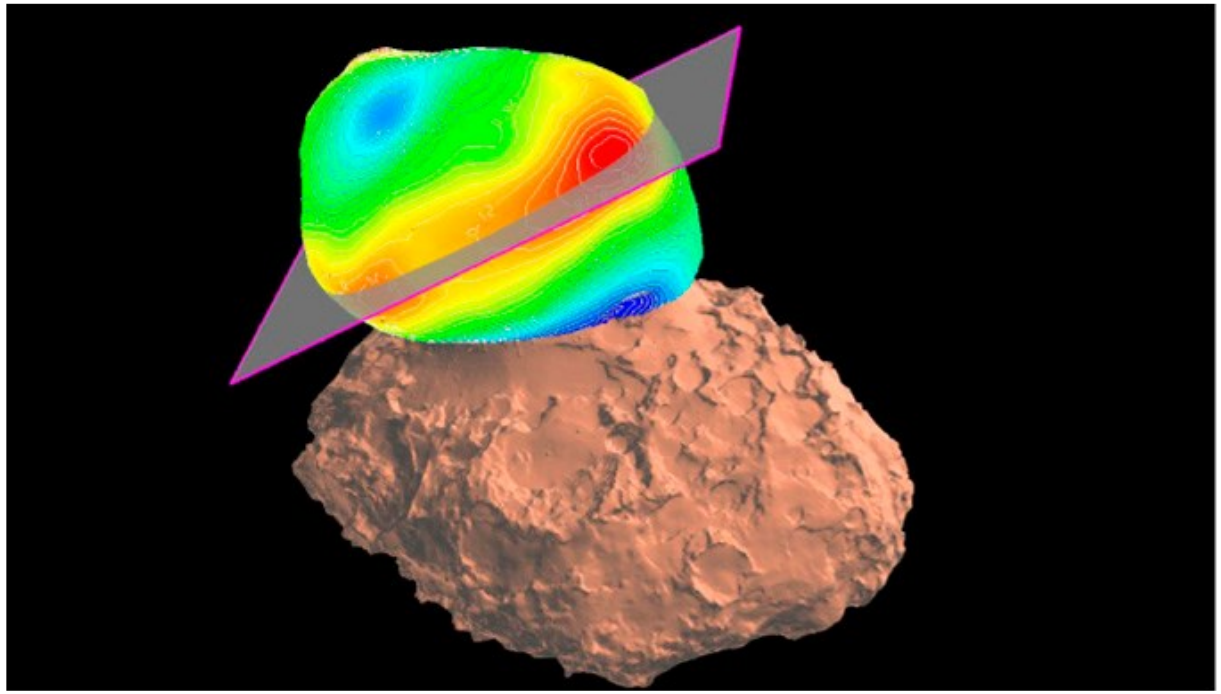

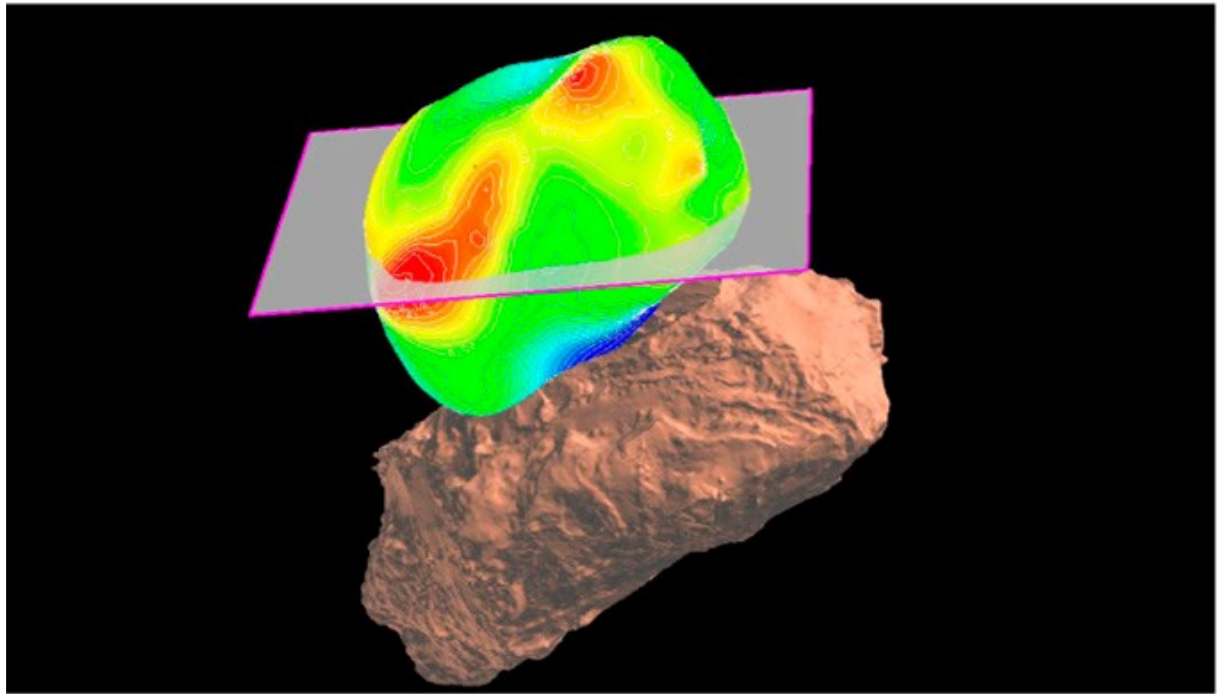

Franceschi et al., 2020

The «average shell» of the implicit layered model of the Small Lobe colored in function of its distance between the «average shell» of the ellipsidal model

Example 5: Comet 67P/Churyumov-Gerasimenko

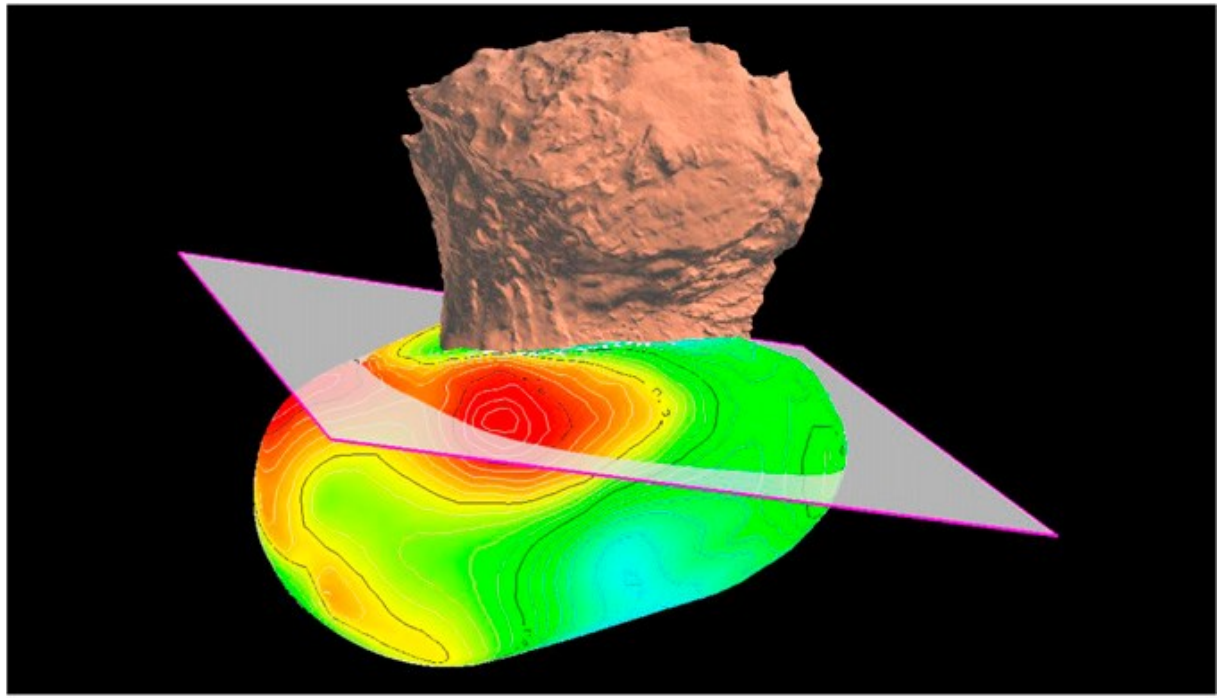

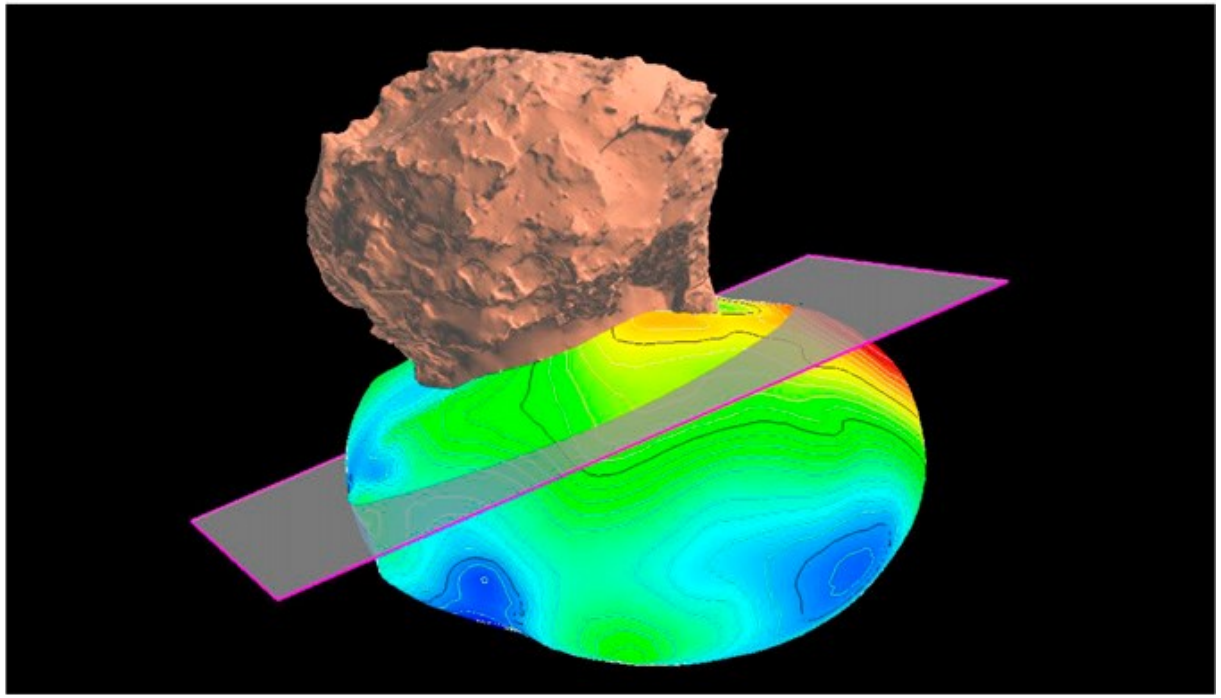

Franceschi et al., 2020

The «average shell» of the implicit layered model of the Big Lobe colored in function of its distance between the «average shell» of the ellipsidal model

Example 5: Comet 67P/Churyumov-Gerasimenko

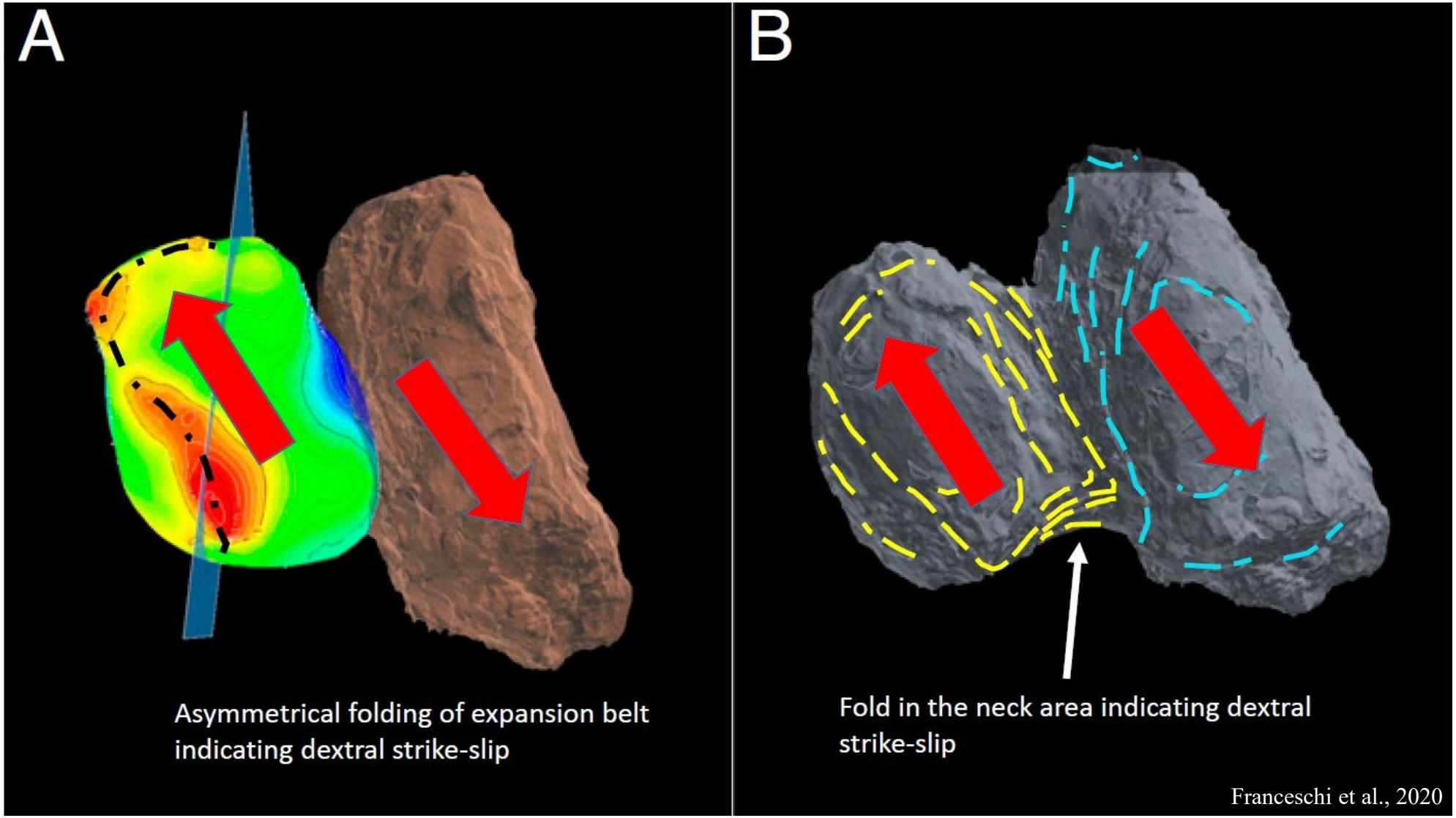

Example 6: outcrop preservation and promotion

VOMs hold great potential for the documentation and digital preservation of significant outcrop that may undergo changes or being destroied.

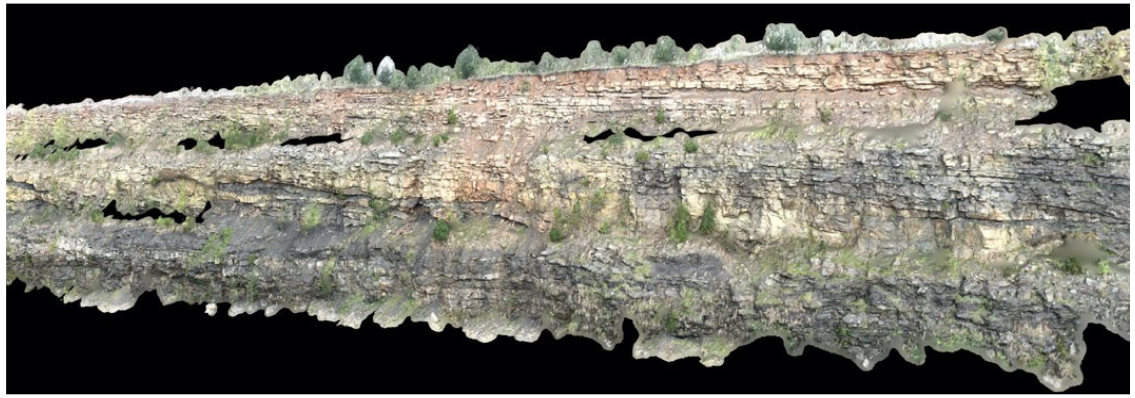

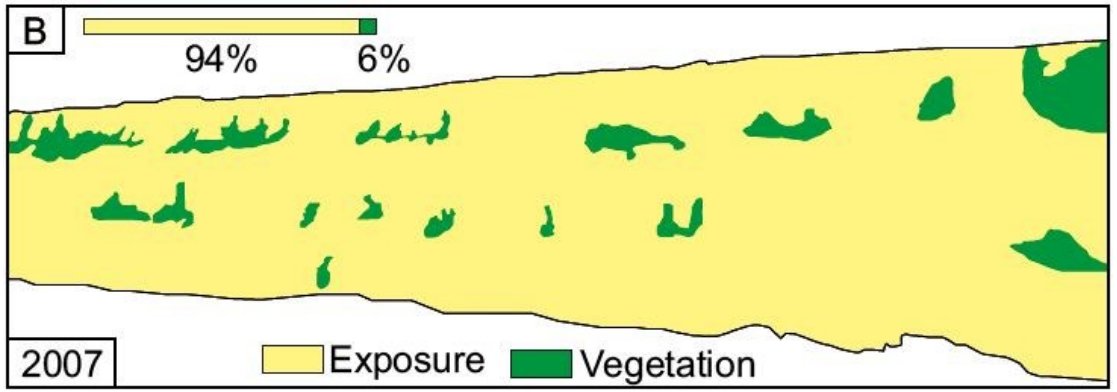

Burnham et al., 2022

Example 6: outcrop preservation and promotion

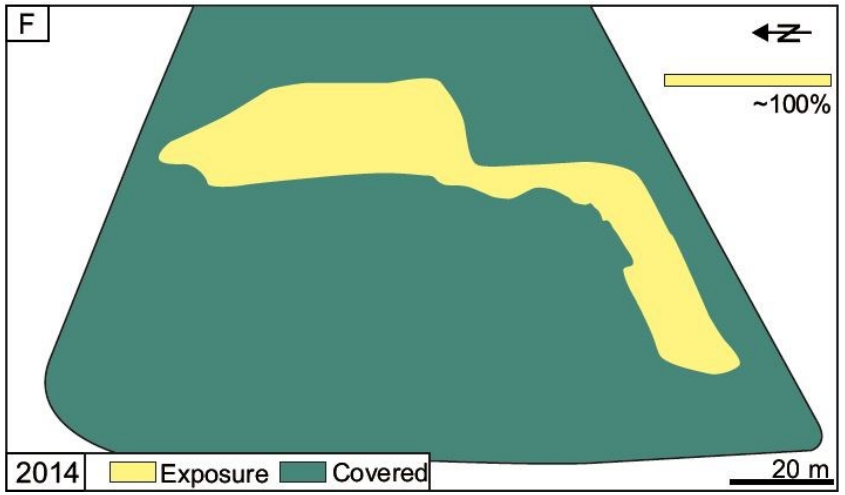

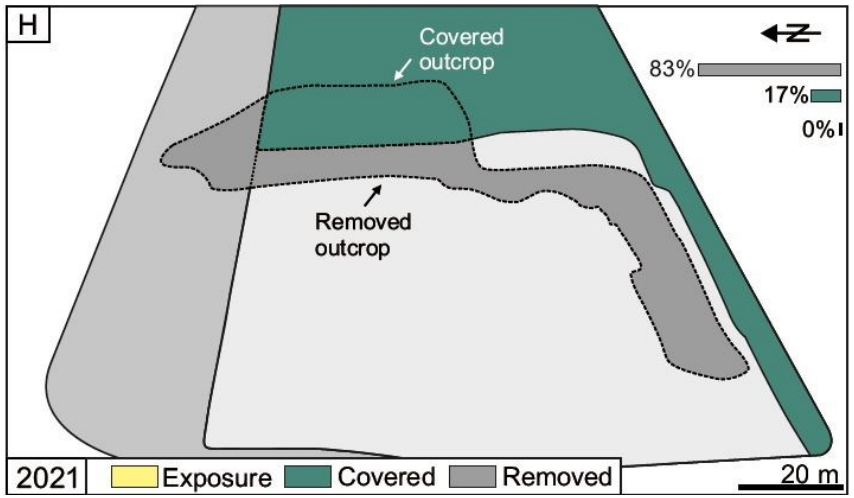

Burnham et al., 2022